AFOSR-TR- 81 -0840

FINAL REPORT

(June 1, 1980 - May 31, 1981)

Prepared for

Air Force Office of Scientific Research
Aerospace Sciences Directorate
Bolling Air Force Base, DC 20332

for

Grant: AFOSR77-3336

INITIATION, COMBUSTION AND TRANSITION TO DETONATION IN HOMOGENEOUS AND HETEROGENEOUS REACTIVE MIXTURES: A SUMMARY

Prepared by

Roger A. Strehlow, Harold O. Barthel, and Herman Krier
University of Illinois at Urbana-Champaign
Department of Aeronautical and Astronautical Engineering

Approved for public release; distribution unlimited
Grant No. AFOSR77-3336 September 1980

UNCLASSIFIED

SECURITY CLASSIFICATION OF THIS PAGE (When Data Entered)

REPORT DOCUMENTATION PAGE	READ INSTRUCTIONS BEFORE COMPLETING FORM
1. REPORT NUMBER: AFOSR-TR- 81-0840	2. GOVT ACCESSION NO.: AD-A109 057
	3. RECIPIENT'S CATALOG NUMBER:
4. TITLE (and Subtitle): INITIATION, COMBUSTION AND TRANSITION TO DETONATION IN HOMOGENEOUS AND HETEROGENEOUS REACTIVE MIXTURES	5. TYPE OF REPORT & PERIOD COVERED: 1 Jun 80 - 30 May 81 FINAL
	6. PERFORMING ORG. REPORT NUMBER:
7. AUTHOR(s): Roger A. Strehlow, H. O. Barthel, Herman Krier	8. CONTRACT OR GRANT NUMBER(s): AFOSR 77-3336
9. PERFORMING ORGANIZATION NAME AND ADDRESS: UNIVERSITY OF ILLINOIS AT URBANA-CHAMPAIGN, AERONAUTICAL AND ASTRONAUTICAL ENGINEERING DEPT, 101 TRANSPORTATION BLDG., URBANA, IL 61801	10. PROGRAM ELEMENT, PROJECT, TASK AREA & WORK UNIT NUMBERS: 61102F, 2308/A1
11. CONTROLLING OFFICE NAME AND ADDRESS: AIR FORCE OFFICE OF SCIENTIFIC RESEARCH/NA, BOLLING AIR FORCE BASE, DC 20332	12. REPORT DATE: Sep 81
	13. NUMBER OF PAGES: 55
14. MONITORING AGENCY NAME & ADDRESS (if different from Controlling Office)	15. SECURITY CLASS. (of this report): UNCLASSIFIED
	15a. DECLASSIFICATION/DOWNGRADING SCHEDULE

16. DISTRIBUTION STATEMENT (of this Report)

Approved for public release; distribution unlimited

17. DISTRIBUTION STATEMENT (of the abstract entered in Block 20, if different from Report)

18. SUPPLEMENTARY NOTES

19. KEY WORDS (Continue on reverse side if necessary and identify by block number)

NON-IDEAL BLAST WAVES
DEFLAGRATION TO DETONATION TRANSITION
INITIATION OF GAS EXPLOSION

20. ABSTRACT (Continue on reverse side if necessary and identify by block number)

This report summarizes the work completed by May 31, 1981 for the Air Force Office of Scientific Research as part of Grant No. AFOSR 77-3336. The research deals with the broad topics of initiation, combustion, and transition to detonation in homogeneous and heterogeneous reactive mixtures. One work area is involved with certain aspects of ignition source effects in reactive fuel-air mixtures. These aspects include effects of chemical sensitizers, flame acceleration, flame area, and ignition point location. The other area involves the hydrodynamic modeling of ignition and flamespreading in granular energetic

DD FORM 1 JAN 73 1473 EDITION OF 1 NOV 65 IS OBSOLETE

UNCLASSIFIED

SECURITY CLASSIFICATION OF THIS PAGE (When Data Entered)

solids to predict the potential for deflagration-to-detonation transition (DDT). Key results in the first area are that chemically sensitized clouds can lead to detonation, that flame acceleration or a large increase in the time rate of increase of the flame area are needed for transition from deflagration to detonation and that it is very difficult to generate damaging over-pressure from edge-ignited combustion even for very high subsonic burning velocities. The research dealing with analysis of DDT in porous high energy solid propellant has shown (for the first time) actual steady-state detonation solutions, following the unsteady flow, for materials with sufficient porosity and critical burning rate properties. Limits of the run-up length to detonation are predicted as a function of propellant chemical energy, burning rate, bed porosity, and granulation (size). The detonation states conform to realistic measured conditions for porous HMX and RDX propellants.

ABSTRACT

This report summarizes the work completed by May 31, 1981 for the Air Force Office of Scientific Research as part of Grant No. AFOSR77-3336. The research deals with the broad topics of initiation, combustion and transition to detonation in homogeneous and heterogeneous reactive mixtures. One work area is involved with certain aspects of ignition source effects in reactive fuel-air mixtures. These aspects include effects of chemical sensitizers, flame acceleration, flame area, and ignition point location. The other area involves the hydrodynamic modeling of ignition and flame-spreading in granular energetic solids to predict the potential for deflagration-to-detonation transition (DDT).

Key results in the first area are that chemically sensitized clouds can lead to detonation, that flame acceleration or a large increase in the time rate of increase of the flame area are needed for transition from deflagration to detonation and that it is very difficult to generate damaging overpressure from edge-ignited combustion even for very high subsonic burning velocities.

The research dealing with analysis of DDT in porous high energy solid propellant has shown (for the first time) actual steady-state detonation solutions, following the unsteady flow, for materials with sufficient porosity and critical burning rate properties. Limits of the run-up length to detonation are predicted as a function of propellant chemical energy, burning rate, bed porosity, and granulation (size). The detonation states conform to realistic measured conditions for porous HMX and RDX propellants.

TABLE OF CONTENTS

RESEARCH OBJECTIVES/STATEMENT OF WORK

The research deals with the broad topics of initiation, combustion and transition to detonation in homogeneous and heterogeneous reactive mixtures. Specific areas of research include the following:

A) Analytical work directed to study direct initiation of detonation by a nonideal blast wave in chemically sensitized reactive fuel-air clouds.

B) An experimental study of non-linear effects upon initiation in a reactive fuel-air mixture with initiation produced behind the Mach stem shock generated on a ramp.

C) An experimental study of the effect of obstacles on flame acceleration in cylindrical geometry and in layered clouds.

D) The numerical and theoretical calculation of the blast waves produced by a centrally ignited spherical source region and application of acoustic monopole source theory and numerical techniques to the deflagrative and detonation combustion of a cloud of arbitrary shape.

E) The DDT phenomenon in granulated propellant or explosives involves a series of complex transient processes that are not well understood at the present time. It is hypothesized that the normal burning process of the solid propellant is disturbed by an abnormality such as a crack in the propellant grain. This abnormality generates regions of porous propellant which can be ignited locally, causing a pressure buildup and formation of a weak shock. If detonation is to be excited following this ignition, it is necessary to ensure a sufficiently rapid pressure buildup. In the case of porous propellant, this may be achieved as a result of the penetration of gaseous combustion products into the interior pores of the solid, which leads to the disturbance of surface burning conditions. Thus, in this case, heat transfer by conduction is replaced by convective heat transfer. Subsequent acceleration of ignition (flame) fronts begins and pressure waves are generated which become shocks. These shocks cause large local over-pressurization and often change into a detonation.

To analyze this phenomenon, the reactive two-phase (solid, gas) conservation equations of continuity, momentum and energy must be solved along with any constitutive relations to account for heat transfer interaction, pressure losses through the aggregate, ignition criteria, unsteady burning

rates, etc. It is only through solutions of such a fluid-mechanics model that one can develop criteria to specify the conditions under which the burning propellant is susceptible to transition to detonation. Considerable effort is involved in developing advanced numerical integration schemes to adequately handle the prediction of strong shock waves in such transient flows.

From the solution of the unsteady two-phase flow model it is possible to assess the important physical and chemical factors that are inherent in the DDT phenomenon. It is then also possible to interpret the experiments where deflagration-to-detonation transition occurs, to assess whether such factors as granulation, compaction, confinement, chemical content, and burning rates can be properly tested.

Experimental research to evaluate the necessary constitutive relations for the momentum and heat transfer in porous beds at high flow-Reynolds number is also underway, since these data represent input to the modeling effort.

STATUS OF THE RESEARCH EFFORT

A. Direct Initiation of Detonation with Chemically Sensitized Clouds.

The question to be answered by numerical calculation was whether the direct initiation of detonation could be generated by an initiating shock wave produced by a proper distribution of a chemical accelerator in a source region within a fuel-air mixture. The reaction was modeled by a modified Arrhenius law of the form,

$$\frac{d\lambda}{d\tau} = A_1 \left[1 + A_2 F(\delta)\right] \frac{(1-\lambda)^n}{v^{n-1}} \exp\left(-\bar{E}^*/\bar{e}\right)$$

where λ is reaction coordinate, A_1 is the dimensionless prefactor for the reaction, A_2 is the accelerator effectiveness factor, $\bar{E}^*$ is the dimensionless activation energy, v and e are dimensionless specific volume and internal energy respectively and n is the order of the reaction. The function $F(\delta)$ is given by

$$F(\delta) = \left[\cos 3\pi\delta - 9 \cos \pi\delta + 8\right]/16$$

where $\delta = \dfrac{R_o - R}{R_o - R_1}$ and R_o is the radius of the core where the chemical accelerator is uniformly distributed and R_1 is the outer edge of the transition zone for the distribution of the chemical accelerator.

A modified Lagrangian time dependent finite difference (Oppenheim CLOUD) program was used in the study. Early efforts using the reaction rate law $\dot{Q} = Q \dfrac{d\lambda}{d\tau}$ where Q is the total energy of the reaction led to such large values of $\dot{Q}$ that it was necessary to limit the maximum value of $\dot{Q}$ in order to keep a sufficiently large time step so the computing time would not become excessive.

Limiting values of the controlling parameters in which transition to detonation occurred were found in 1978 for this model. Subsequently in 1979 we sought to investigate the effect of a more rapid cutoff in reaction rate below 1000 K. Our curve for the logarithm of reaction rate versus inverse temperature puts the "knee" at 1000 K and contains a parameter which shifts the value of the rate at the knee. As we reduced the value

of this parameter the reaction zone became so narrow that it encompassed only one cell. Therefore, we sought to modify the CLOUD program by subdividing a band of cells which moved with the reaction front. A linear curve fit led to numerical calculation instabilities and a cubic spline function fit permitted some extension of the range, but we have not been able to solve the problem satisfactorily.

Besides the annual reports to the contractor, this work led to the publication: H. O. Barthel, and R. A. Strehlow, "Direct Detonation Initiation by Localized Enhanced Reactivity," AIAA Paper, 79-0286 (1979).

B. Nonlinear Effects

The nonlinear initiation experimental program in 1977-1978 used, as a geometry for reflected shock initiation under non-uniform conditions, a 15^{o} ramp at the end of the shock tube placed just before the shock hits the back wall. The Mach stem shock would generate, when reflected, a temperature behind it approximately 100 K higher than the bulk gas reflected temperature due to the normal shock reflection of the incident shock. The initial shock strength was adjusted so that the normal reflected shock temperature lies in the range from approximately 900-1200 K on different shots, and therefore the ratio of time delays in the regions behind the reflected normal and reflected Mach stem shocks could be adjusted over a large range because of the nonlinear behavior of the slope of the induction delay curve versus 1/T in this temperature regime. The program was less than successful, for we did not obtain meaningful smoked foil records and had to resort to pressure records to determine that transverse initiation occurred on some runs. The results appear in the report by John K. Soldner, "Direct Initiation of Detonation Using Finite Amplitude Wave Acceleration," MS thesis, University of Illinois, 1978.

C. Propagation of a Flame in a Layered Propane-Air Mixture

In connection with the development of monopole source theory for the deflagrative combustion of a cloud of arbitrary shape (this will be discussed in the next section), it was necessary to determine how rapidly a flame propagated in a layered cloud under conditions where it was edge-ignited. For this purpose a 80 cm by 80 cm aluminum plate

was mounted at a 10 degree angle to the horizontal and a 8 cm by 8 cm by 20 cm high chamber was filled with a combustible propane air mixture and mounted on the top edge of this plate. When this chamber was tilted the propane-air mixture poured out over the plate. A torch was mounted at the lower edge of the plate and when the propane-air mixture reached the torch, it flashed back to the source. Schlieren photographs were made to determine the flame propagation velocity. It was found that the flame propagated at about 3 to 3½ times the maximum normal burning velocity for a propane-air mixture. This information was used to construct the theory which will be discussed in a later section (see section D).

Propagation of a flame in a 2-dimensional layered mixture

Preliminary to the study of the effect of obstacles on flame acceleration an apparatus was built which was 10 cm wide, 50 cm long and 15 cm high containing a bottom plate of aluminum with a bronze insert to allow the infusion of combustible mixtures, two-side glass walls and an endplate containing 5 spark gaps for ignition. On the opposite side of the endplate a gate was placed which was used to control the layer height and was dropped out of position just before the sparks were fired. This apparatus was used to determine flame propagation behavior and the effect of the buoyancy vector on flame propagation using methane-air and propane-air mixtures. (Methane-air is lighter than air and therefore the apparatus was mounted upside down for the methane tests). The preliminary results of these tests as well as the tests on flame propagation over the inclined plate are reported in a master's thesis by P. G. Huseman, dated 1980, entitled, "Two and Three Dimensional Unconfined Flame Studies."

D. Theoretical Analysis of the Blast Wave Produced by Deflagrative and Detonative Combustion of Spherical and Non-spherical Source Regions

The work reported in this section has resulted in a rather complete understanding of the manner of which source behavior affects the blast wave under detonative or deflagrative combustion in the source region. The first paper entitled 'The Blast Wave Generated by Spherical Flames," by R. A. Strehlow, R. T. Luckritz, A. A. Adamczyk and S. A. Shimpi,

Combustion and Flame, 35, pp. 279-310 (1979), contains a complete description of the effect of a spherically expanding flame with various normal burning velocities up to detonative combustion on the blast wave generated around a spherical source region. The effect of flame acceleration was also studied by arbitrarily legislating certain types of acceleration processes and studying their effects. Additionally, for low velocity flames, Taylor's theory for the blast wave produced by a constant velocity spherical piston was adapted to flame propagation and was found to fit the numerical calculations quite well.

Subsequent to that work a principle first enunciated by Stokes in 1849 was adapted to deflagrative combustion of clouds of arbitrary shape. This led to a paper entitled, "The Blast Wave from Deflagrative Explosions; An Acoustic Approach," by R. A. Strehlow, 14th Loss Prevention Symposium, AIChE, p. 145 (1981). This paper shows that deflagrative combustion of clouds of large aspect ratio with edge ignition yields blast pressures which are considerably lower than blast pressures produced by a flame propagating at the same velocity as a spherical flame from the center of a source region. Experimental verification for this effect was found in the open literature.

An extension of this work on a sounder theoretical foundation is being performed by M. S. Raju at the present time. Mr. Raju has developed a rather simple hydrocode which does not give a great deal of detail but nevertheless allows one to calculate pressures and flow velocities as well as shock wave positions for blasts from deflagrative or detonative combustion of clouds of arbitrary shape (with cylindrical geometry). This program will lead to a Ph.D thesis which will be published in the open literature.

The above work on deflagrative and detonative explosions in the open has shown quite definitely that damaging blast waves cannot be obtained from ordinary deflagrative explosions. Instead, one needs either a detonative explosion or some type of high velocity volumetric combustion process to occur before a damaging blast wave will be generated when a vapor cloud burns. This information, coupled with the SWACER mechanism recently discovered by John Lee and his co-workers at McGill, leads one to the conclusion that the really damaging vapor cloud explosions are due to detonative behavior in the cloud.

In addition to the above work, a paper entitled, "Accidental Explosions," was published by Roger A. Strehlow in the American Scientist magazine, July-August, (1980). This paper represents a generalized summary of the behavior of all types of accidental explosions and a logical characterization of them into 9 catagories.

E. Modeling of DDT in Porous High Energy Propellants

The reactive two-phase flow modeling to study the transition potential of high energy, but porous solid propellant to a steady detonation wave has for the first time shown that a detonation solution is possible. This represents a major achievement, since until this year, no such solutions were ever shown. Improvements in the analysis which contributed to the successful DDT modeling included:

(a) several significant advances in the numerical integration techniques to handle extreme shock wave formation;

(b) use of more appropriate dynamic gas permeability constitutive relations, based on AFOSR supported research under this grant;

(c) utilization of improved shock Hugioniot data for HMX detonation products, thereby modifying both the non-ideal gas phase and solid phase equations of state.

Appendix A is a copy of a paper (to appear in Combustion and Flame) which summarizes our results for the DDT modeling effort. The paper was condensed from a recent AFOSR Interim Report (Univ. of Illinois Tech. Report AAE 81-1), by P. Barry Butler and H. Krier, entitled, "Shock Development and Transition to Detonation Initiated by Burning in Porous Propellant Beds." The paper presents solutions which indicate clear regimes for detonation potential. Predictions for the run-up length to detonation are shown bounded as a function of either propellant chemical energy content, propellant burning rate, bed porosity, or particle size (granulation). Comparison of DDT with limited data available in the literature indicates good qualitative agreement with many of these predictions and exceptionally good quantitative agreement with detonation pressure and detonation speeds, as a function of propellant bulk density and propellant energy.

F. Measurements of Gas Permeability in Packed Beds

This past year additional experiments have been carried out that extend the range-of-validity of the packed-bed gas-permeability friction coefficient, a relation of prime use in the gas dynamics associated with the DDT modeling. This correlation was tested on both data obtained in our laboratory, as well as data (downstream pressure decrease in packed beds of solid particles) from other laboratories.

The gas permeability correlation matches the relatively low Reynolds number conditions of published work in the literature, but clearly indicates that one should not extend those conventionally used correlations to relatively high Reynolds number conditions. Basically, our correlation indicates that the bed is significantly more permeable than would be predicted by using classical correlations (generally found in the chemical engineering literature). A technical paper is currently being written for submission to a journal in the open literature which will summarize our findings in this area.

Dynamic measurements of high pressure decay through packed beds were also made using a blow-down air facility, so that the initial pressure decayed from 2500 psia (17.2 MPa) to 100 psia (0.69 MPa) in a matter of several seconds. The transient test data indicate that our steady-state gas permeability correlation was still valid for this type of dynamic event. Although transient gas permeability data in sub-millisecond times would best confirm to our DDT flow modeling regime, we believe that until such tests are made the gas-particle drag correlation now in use represents the best state-of-the-art relation.

NEW DISCOVERIES

A. Reactive Gas-Air Mixtures

1. Direct initiation of detonation in numerical simulation can be achieved by proper distribution of a chemical accelerator in a reactive fuel-air cloud.

2. Limiting values of the controlling parameters in the chemical accelerator model exist.

3. Source behavior affects the possibility of transition to detonation.

4. Either large flame area rate increases or flame accelerations are needed to cause transition to detonation.

5. Edge ignition provides so much lateral relief that relatively low blast pressures are produced.

6. Ordinary deflagrative sources should not produce severely-damaging blast waves.

B. High Energy Propellants

1. For the first time complete deflagration wave to detonation wave transition has been shown as a solution to the reactive gas-solid dynamics model of the flow physics.

2. Detonation solutions require critical values of chemical energy, bed porosity, propellant pyrolysis rates, and particle granulation.

3. Solid particle compressibility is a requirement in order to achieve DDT in moderate porosity propellant.

4. The burning-rate pressure index of high energy propellants should not exceed values of 3/4 for HMX energy levels and average particle sizes greater than 250 μm in diameter. Detonation is not predicted for indices, n, less than 0.80, for cases studied to date.

5. For high energy propellants, packed to porosities, ϕ_o, ranging from 0.25 to 0.50, no detonation transition is predicted if the average particle size is greater than 500 μm (½ mm). Hence, friable propellants should be avoided to preclude DDT hazard.

CUMULATIVE CHRONOLOGICAL LIST OF WRITTEN PUBLICATIONS IN TECHNICAL JOURNALS

1. "Accidental Explosions," by Roger A. Strehlow, American Scientist, July-August (1980).

2. "The Blast Wave Generated by Spherical Flames," by R. A. Strehlow, R. T. Luckritz, A. A. Adamczyk, and S. A. Shimpi, Combustion and Flame, 35, pp. 297-310 (1979).

3. "The Blast Wave From Deflagrative Explosions: An Acoustic Approach," by R. A. Strehlow, to be published in the 13th Loss Prevention magazine AIChE (presented in Philadelphia, PA, June 11, 1980).

4. "Modeling of Unsteady Two-Phase Reactive Flow in Porous Beds of Propellant," by S. S. Gokhale and H. Krier; to be published in Progress in Energy and Combustion Science, (Nov. 1981).

5. "Fluid Mechanics of Deflagration-to-Detonation Transition in Porous Explosives and Propellants," AIAA paper 80-1205; by S. J. Hoffman and H. Krier; to be published in AIAA Journal (Nov. 1981).

6. "Modeling of Shock Development and Transition to Detonation Initiated by Burning in Porous Propellant Beds," by H. Krier, P. B. Butler, and M. F. Lembeck; to appear in Combustion and Flame (Dec. 1981).

PROFESSIONAL PERSONNEL ASSOCIATED WITH THE RESEARCH EFFORT

(A) 1) Prof. Roger A. Strehlow

2) Prof. Harold O. Barthel

Graduate Students

a) Mr. M. S. Raju
Ph.D. candidate (current)

b) Mr. J. K. Soldner
M.S. Thesis (1979); entitled "Direct Initiation of Detonation Using Finite Amplitude Wave Acceleration"

c) Mr. P. G. Huseman
M.S. Thesis (1980); entitled "Two and Three Dimensional Unconfined Flame Studies"

d) Mr. S. A. Shimpi
Ph.D. Thesis (1979); entitled "The Blast Wave Produced by Bursting Spheres with Simultaneous or Delayed Explosion or Implosion of the Contents"

(B) 3) Prof. Herman Krier

e) Mr. P. Barry Butler
Ph.D. candidate (current)
M.S. Thesis (1981); entitled "Shock Development and Transition to Detonation Initiated by Burning in Porous Propellant Beds"

f) Mr. S. S. Gokhale
Ph.D. Thesis (1980); entitled "Theoretical Studies in Two-Phase Flow Prior to the Transition to Detonation in Granular Solid Propellants"

g) Mr. S. J. Hoffman
M.S. Thesis (1980); entitled "Fluid Mechanical Processes of DDT in Beds of Porous Reactive Solids"

h) Mr. S. F. Wilcox
M.S. Thesis (1980); entitled "Gas Flow Measurements Through Packed Beds at High Reynolds Numbers"

i) Mr. M. Lembeck
Graduate Assistant

APPENDIX A:

MODELING OF SHOCK DEVELOPMENT AND TRANSITION TO DETONATION INITIATED BY BURNING IN POROUS PROPELLANT BEDS

by

H. Krier, P. B. Butler, M. F. Lembeck
Department of Mechanical and Industrial Engineering
University of Illinois at Urbana-Champaign

ABSTRACT

This paper deals with the analyses of deflagration to detonation transition (DDT) occurring in a packed bed of granular, high energy solid propellant. A reactive two-phase flow model of this phenomena is solved by utilizing a Lax-Wendroff finite differencing technique. Utilizing an appropriate gas phase nonideal equation of state and high pressure gas permeability relations with an improved numerical integration technique, one can predict the transition to a steady detonation from initiation by deflagration.

Analyses are presented that clearly indicate the effect of the propellant physical and chemical parameters on the predicted run-up length to detonation. Predictions of this run-up length to detonation are presented as a function of propellant chemical energy, burning rate, bed porosity, and granulation (size). Limited comparison with actual DDT data in the literature indicates qualitative agreement with these predictions.

To appear in Combustion and Flame (December 1981)

INTRODUCTION

This paper summarizes the analysis associated with the accelerating deflagration wave in a porous medium of reactive solid propellant. The hazard of DDT (deflagration-to-detonation transition) in solid propellants, especially solid propellants burning in rocket motor environments, is usually not considered a possibility. However, it may be that under certain situations (for example, a grain structure failure) the solid motor may crack and form regions of granular or porous propellant. When flame from the surface-deflagrating propellant reaches this seam of porous material it will accelerate into this medium and be supported by convective heat transfer from the burned gas into the unignited porous region. If, in addition to this, the product gases are confined to a finite volume, the accelerating deflagration could transit into a detonation. Propellants exhibiting a high chemical energy per unit mass and capable of rapidly generating gases through their burning rate are more likely to experience this type of deflagration to detonation transition.

Analysis of the flows in such an unsteady two-phase mixture is a complicated exercise. Work has been underway at the University of Illinois since 1976 to develop a reactive hydrodynamic code in which the combustion of porous propellants can be modeled in such a way as to predict the behavior of a corvectively driven flame in a confined situation. Details of these modeling exercises are found in Ref. 1-4. In an evolutionary manner this work included the formulation of the two-phase flow conservation equations, first assuming that the mixture was a continuum, and at a later date treating each phase as a separate continuum irrespective of the mixture properties. The most recent analysis of the unsteady two-phase

flows associated with, but prior to, DDT is documented in the paper by Hoffman and Krier [3]. This work, therefore, represents the starting point for the study that is presented here.

The reader, after reviewing the above noted reference, can easily see that the modeling of this transient phenomena utilizes a number of important constitutive relations which form closure of the conservation equations. For example, one must have information on the burning rate of the material that is a function of the surrounding pressure and temperature. One also requires expressions for the dynamic gas permeability and the subsequent heat transfer rates of the hot gases as they are forced into the unignited porous material. In addition, relations which represent the resistance to compaction of the solid matrix must be included. Equations of state, not only for the high pressure in the product gases, but also for the solid itself, must be supplied (as shown in Ref. 3). The assumption of an incompressible solid, although providing some reasonable answers as far as the deflagration speed, is <u>not</u> an accurate indicator of the peak pressures that are possible during the accelerating deflagration mode. Since these pressures are precursors to the final detonation solutions that would be expected, it is clear that a compressible solid must be modeled.

The analysis of the DDT problem requires the solution of the time-dependent conservation equations for both particle and gas phases and the necessary constitutive relations noted above. The conservation equations form a system of nonlinear hyperbolic equations, which require numerical finite differencing schemes. A recent report has summarized several of these integration shcemes and evaluated which are most useful for this type of reactive flow [5].

Previous Results on DDT Modeling

A review of Refs. 2-4 indicates that a steady state detonation solution was not a predicted result. Based on the steady shock hydrodynamics for a "homogeneous" reactive material with a known chemical energy, initial solids loading and material parameters, a steady state detonation (CJ) would propagate at speeds of the order of 5-8 mm/μsec, with a detonation pressure of the order of 12-20 GPa [5]. Although a fairly rapid flame front, often approaching a steady state speed of 2 mm/μsec, was typical of the solutions presented in the work by Gokhale and Krier[2], Kezerle and Krier [4], and Hoffman and Krier [3], the associated peak pressures were never of significant manner to suggest that these final flame spreading rates were characteristic of an actual detonation. Although the peak pressures predicted in Refs. 2-4 ranged between 1/2 to 5 GPa and were consistent with such velocities, these pressures could not represent the detonation (CJ) pressures.

Continued work (which is reported here) indicates that it is now possible to obtain a detonation solution, but in order to do so a number of important modifications and corrections to the work reported in Refs. 2-4 were required.

DDT in Two-Phase Reactive Flow (Experimental Data)

The transition from deflagration to detonation in a porous reactive medium is an unsteady process. Hot gases generated from the propellant surfaces are driven forward into the unburned solid matrix by the pressure gradient developed at the ignition front. This phenomena is not found when a nonporous solid detonates, since only pressure disturbances can be propagated ahead of the ignition front. It is this convective heat transfer

to the unignited propellant and the extended deflagration reaction zone, with the resultant compression of the solid, which makes DDT in a porous bed unique when comparing it to DDT in either an all gas or an all solid regime.

Much experimental work on DDT in porous material has been carried out in the past decade. Bernecker and Price have published their earliest detailed results on DDT in Refs. 6 and 7. Other experimental studies prior to these include the work of Griffiths and Grocock [8] and Taylor [9].

The work presented in Ref. 7 by Bernecker and Price is a study of DDT in RDX (cyclotrimethylenetrinitramine), a shock sensitive high-energy explosive. In their experiments the RDX was packed into a thick walled tube having an inside diameter of 16 mm and being approximately 300 mm (12 in.) in length. Both ends of the column were closed and ionization probes were located throughout the bed to trace the ignition front locus. The RDX was packed in an inert wax mixture and had a mean particle size of 200 μm in diameter.

Their experimental work showed a convective ignition front traveling at subsonic velocities (0.3-0.9 mm/μsec) for most cases when the initial porosities, ϕ_o, ranged between values of 0.1 to 0.3 and in cases where transition occurred, detonation velocities ranged from 6-8 mm/μsec. The length of porous propellant required for compressional waves to overtake the ignition front and transit into a detonation was defined as ℓ_{CJ}, the run-up length. Typical values for ℓ_{CJ} ranged from 100 to 200 mm.

THE MODEL AND ANALYSIS

Introduction

The analysis that follows attempts to model the situation in which a bed of tightly packed granular propellant is ignited at one end. Both ends of the packed bed are considered closed, thus treating the problem when the velocity of the rear wall is much less than the CJ product velocity. For this case, after DDT, the detonation propagates through the unignited region at the CJ detonation velocity and detonation pressure and is followed by an isentropic expansion of the gases to the pressure at the stationary wall. The gas surrounding the particles at the initial time is considered inert, and to be at atmospheric pressure. It is also assumed that the inert gas will fully mix with the gases being generated from combustion of the propellant as time progresses.

For numerical simplicity the propellant particles are assumed to be unisized spheres. Particles of interest range in diameter $50\mu m < d_p < 200\mu m$. To treat multi-sized particles, one would require $\underline{N}$ independent equations of mass, momentum and energy for the solid phase, where $\underline{N}$ is the number of initially different-sized particles. A solids loading of 74% is the tightest possible for unisized spheres, obtainable by arranging the spheres in a face centered cube. However, assuming granular deformation occurs under high stress loads, greater solids loadings may be predicted without error. Obviously, the spherical geometry must be altered for this to occur.

As the small fraction of propellant particles ignited at time t=0 burn, hot gases are generated as a function of the pressure-dependent burning rate law and surface-to-volume ratio ($3/r_p$) of the spheres. These hot gases are convected forward through the lattice of unburned

propellant and flow gradients develop, as dictated by the solution of the conservation equations and the necessary constitutive relations.

Heat transfer from the hot gases to the unignited propellant particles, dependent on the velocity of the gas relative to the particles and several gas properties (i.e. viscosity, thermal conductivity), transports energy from the gas to the solid phase. Subsequent ignition of particles further down the bed is assumed to occur when a critical solid phase internal energy is reached [2]. This energy can be expressed as a critical increase in solid phase temperature, T_p, since the specific heat of the solid is assumed to be known.

As time progresses the gas pressure behind the ignition front increases due to the confinement of the gases from the closed rear boundary and the pressure-dependent rate of mass generation in the gas phase. Under certain conditions* the pressure gradient can develop into a shock front which overtakes the ignition front propagating through the bed. When this occurs the ignition front experiences the transition from deflagration to detonation.

At the transition point the ignited region (zone of gas generation) narrows in width and is followed by a region of all gas where the propellant particles are completely burned out, as depicted in Figure 1. The thickness of the reaction zone is a function of the initial particle size and solids loading, and thicknesses approaching 1mm may be possible as $r_p \to 0$ and $\phi_o \to 0$.

---

* These conditions will depend upon the solid chemical energy, granulation (size and loading), burning rate, ignition energy, etc.

Assumptions

In order to numerically model DDT in two-phase flow, while retaining the physics of the problem, several key assumptions had to be made. These assumptions are similar to those made by previous investigators (Refs. 2 and 4):

(1) Both the solid and gas phases are independently treated as continuums requiring their own conservation relations.

(2) Each phase interacts with the other. This is modeled by the mass, momentum and energy interaction terms in the conservation equations.

(3) All propellant particles are unisized spheres.

(4) Ignition of a propellant particle is obtained when a critical energy, expressed as a particle temperature, is transferred to the solid.

(5) The propellant particles are initially surrounded by an inert gas at temperature, T_{g_o}.

(6) During combustion of the propellant, the gaseous products mix with the inert gas described in assumption #5.

(7) Both ends of the bed are closed allowing no gases to escape.

(8) The specific heats at constant volume, C_v, for both phases are constant.

(9) When the solid phase, at a given x-location in the bed, displays a porosity $\phi > 0.98$ and a particle volume less than one-tenth of its initial volume, it is burned out and no longer generating gas. Results show this phenomena to proceed smoothly from the left boundary and thus not leaving any 'holes' in the continuum.

This assumption was necessary to prevent a singularity from arising as $r_p \to 0$ and $\Gamma \to \infty$.

(10) All the product gases obey an assumed nonideal equation of state, which is reviewed in detail below.

(11) The solid particles are compressible, without heating up, obeying a modified Tait equation of state.

(12) Once ignited, the particles are assumed to burn on the outer surface only, at a known pressure-dependent rate law.

(13) At some initial time, a "narrow" region at one end is ignited, burning at the low pressure prescribed.

Governing Equations

Numerical modeling of the two-phase reactive flow process in DDT involves the conservation of mass, momentum and energy per unit volume in both gas and solid phases. This is a system of six conservation conditions which form a set of nonlinear hyperbolic partial differential equations coupled by the interphase mass, momentum and heat transfer terms (Γ, $\mathcal{D}$, Q). The conservation equations for two-phase reactive flow have been developed previously and Refs. 3 and 4 will provide the reader with the definitions, assumptions and expressions for the six following field-balanced conservation equations. Also, Appendix A will provide an explanation of the interphase transfer terms.

Gas Continuity

$$\frac{\partial \rho_1}{\partial t} = - \frac{\partial (\rho_1 u_g)}{\partial x} + \Gamma \qquad (1)$$

Particle Continuity

$$\frac{\partial \rho_2}{\partial t} = - \frac{\partial (\rho_2 u_p)}{\partial x} - \Gamma \tag{2}$$

Gas Momentum

$$\frac{\partial (\rho_1 u_g)}{\partial t} = - \frac{\partial (\rho_1 u_g^2)}{\partial x} - \phi \frac{\partial P_g}{\partial x} - \mathcal{D} + \Gamma u_p \tag{3}$$

Particle Momentum

$$\frac{\partial (\rho_2 u_p)}{\partial t} = - \frac{\partial (\rho_2 u_p^2)}{\partial x} - (1-\phi) \frac{\partial P_p}{\partial x} + \mathcal{D} - \Gamma u_p \tag{4}$$

Gas Energy

$$\frac{\partial (\rho_1 E_{g_T})}{\partial t} = - \frac{\partial (\rho_1 u_g E_{g_T} + \phi u_g P_g)}{\partial x} + \Gamma \left[E^g_{CHEM} + \frac{u_p^2}{2} \right] - \mathcal{D} u_p - \dot{Q} \tag{5}$$

Particle Energy

$$\frac{\partial (\rho_2 E_{p_T})}{\partial t} = - \frac{\partial (\rho_2 u_p E_{p_T} + (1-\phi) u_p P_p)}{\partial x} + \Gamma \left[E^p_{CHEM} - \frac{u_p^2}{2} \right] + \mathcal{D} u_p + \dot{Q} \tag{6}$$

Here, the relations for the total internal energy in each phase are

$$E_{g_T} = C_{v_g} T_g + \frac{1}{2} u_g^2 \quad \text{and} \quad E_{p_T} = C_{v_p} T_p + \frac{1}{2} u_p^2 \tag{7}$$

The subscripts g and p denote gas and particle respectively. In Eqs. 1 to 6, the phase densities, ρ_1 and ρ_2, are defined as

$$\rho_1 = \rho_g \phi \qquad \text{and} \qquad \rho_2 = (1-\phi)\rho_p \tag{8}$$

The porosity, ϕ, is defined as the ratio of the instantaneous gas volume to the mixture volume. Hence, the solids fraction is $(1-\phi)$.

In addition to the six conservation equations, three constitutive relations are needed in order to solve for the nine unknown variables; ρ_g, ρ_p, u_g, u_p, T_g, T_p, ϕ, P_g and P_p. These relations include state equations for both gas and solid states and a stress-resistance relation for P_p. Appendix A gives a complete listing of the relations use.

Improvements in Modeling

Since the work reported in Ref. 3, certain "improvements" in the modeling effort have allowed solutions which may be considered to be actual detonations. These improvements are discussed in some detail later in the text, but basically include:

1. Implementation of the necessary gas phase (nonideal) equation of state, to insure that at the CJ (Chapman-Jouget) conditions, the isentrope provides for a "gamma law" suitable at the hydrodynamic CJ state.
2. Implementation of a new gas-particle friction coefficient, as developed by Wilcox and Krier [10], for flows at the high Reynolds numbers encountered in the developing DDT flows. Previously such coefficients were based on data only available for moderate Reynolds number ranges.

3. Utilization of an improved numerical integration scheme, which allowed for a reduction in the grid spacing (and hence reduction of the time increment) without the usual penalty of excessive computation costs and numerical instability that often follows when the total number of integrations is significantly increased. Details are documented in a recent report by Butler and Krier [5].

Equations of State: Constraint Due to the Detonation State

As has been mentioned, a nonideal equation of state must be utilized for the product gases. The analysis presented here uses a nonideal equation of state for hard spheres suggested by S. J. Jacobs [11]. Previous to this study, a covolume-type state equation with data made available by Cook [12] was used (see discussion in Ref. 2).

The hard sphere equation of state takes the form

$$\frac{Pv}{RT} = 1.0 + b\rho + c\ (b\rho)^2 + \ldots \qquad (9a)$$

where the constants b and c are determined by the value of the gamma law coefficient, γ, for the product gases. Here, γ is the negative logarithmic slope of the isentrope tangent to both the Rayleigh and Hugoniot lines at the CJ point in the detonation state. That is, the slope of the isentrope that the gases expand along in the product state. The reader may refer to Ref. 5 for the complete solution of the constants b and c.

Values for γ range from two to three for detonating high density explosives [13]. For the baseline case considered in this study, a value of $\gamma = 2.05$ was selected and the corresponding nonideal equation of state is:

$$\frac{Pv}{RT} = 1.0 + 2.5\ \rho_g - 0.50\ \rho_g^2 \qquad (9b)$$

When the above coefficients (2.5 and 0.50) were altered to treat a case for $\gamma = 3.0$, excessively high gas and particle temperatures were predicted, as one might expect. In addition, during the numerical integration, severe oscillations in gas and particle temperatures occurred in most cases when $\gamma > 3$. Since one is always constrained by the numerical integration schemes that are employed to handle very severe gradients in the flow, it is understandable that previous efforts in DDT modeling [2, 3], which were utilizing such high γ values for the product gases, almost always ran into numerical integration problems. For example, evaluating the covolume state equation previously used in Ref. 3, a value of $\gamma = 3.6$ is calculated. This large value for γ may be one important reason why the calculations, as reported in Refs. 2-4, were unable to handle the high pressures associated with steady state detonations.

In the solid phase the particles obey a modified Tait equation allowing for compression of the granules. This is written as:

$$\rho_p = \rho_{p_o} \left[\frac{3P_p}{K_o} + 1\right]^{1/3} \qquad (10)$$

where K_o is the bulk modulus. Ref. 3 discusses the Tait equation in more detail. A typical value is $K_o = 1.38$ GPa (2.0×10^5 psi).

CJ (Detonation) State

In the text by Fickett and Davis [13] equations are presented for estimating detonation velocity, D_{CJ}, and the detonation pressure, P_{CJ}, for a steady state detonation. These are given for a single phase explosive:

$$P_{CJ} = 2(\gamma-1)\rho_{p_o} E_{CHEM} \tag{11}$$

and

$$D_{CJ}^2 = 2(\gamma^2-1) E_{CHEM} \tag{12}$$

Here, ρ_{p_o} is the initial solid material density and E_{CHEM} is the chemical energy liberated by burning the solid. Since the problem being considered is two-phase (solid-gas), Eqs. 11 and 12 must be modified to account for this by converting ρ_{p_o}, the initial solid density, to ρ_{2_o}, the initial solid phase density $\rho_{2_o} = \rho_{p_o}(1-\phi_o)$. For an initial solid density $\rho_{p_o} = 1994$ kg/m^3, an initial porosity $\phi_o = 0.30$, a chemical energy $E_{CHEM} = 5.48$ MJ/kg, and assuming $\gamma = 2.05$, Eqs. 11 and 12 give respectively: $P_{CJ} = 16.06$ GPa and $D_{CJ} = 5.92 \frac{mm}{\mu sec}$.

These equations were developed from the jump equations for one-phase flow where the equation of state for the product gases was assumed ideal. Because of this, the above values should be considered only as good estimates for the detonation pressure and velocity.

Gas Permeability

One of the key constitutive relations required in the analysis is the gas-particle (interphase) viscous force, which governs hot gas penetration into the unignited region of the granular material. As presented in Appendix A:

$$\mathcal{D} = \frac{\mu_g}{4r_p^2}(u_g - u_p) f_{pg} \tag{13}$$

where f_{pg} is the drag coefficient. Until recently, the packed bed correlations by Ergun or Kuo and Nydegger (as reviewed in Ref. 10) were utilized for f_{pg}. Thus, the modeling efforts presented in Ref. 3 and 4 used

the expression of Kuo and Nydegger [15]:

$$f_{pg} = \frac{(1-\phi)^2}{\phi^2} \{276 + 5 \left(\frac{Re}{1-\phi}\right)^{.87}\} \quad (14)$$

Eq. 14 was developed for $460 < Re < 14{,}600$. Here, Re is the appropriate Reynolds number, defined as:

$$Re = [(\phi u_g)\rho_g \, 2r_p]/\mu_g \quad (15)$$

Based on experiments at both high gas velocities and high Reynolds numbers, Wilcox and Krier [10] developed the correlation:

$$f_{pg} = 5.06 \times 10^5 \, r_p \, Re/u_g^2 \quad (16)$$

where u_g is given in m/sec, r_p in meters, and the constant 5.06×10^5 must have units of m/s^2. This expression is not valid for either very low gas velocities, since Eq. 16 would give $f_{pg} \to \infty$ as $u_g \to 0$, or for very high gas velocities*, since $f_{pg} \to 0$ as $u_g \to \infty$. The equation was found to be fairly accurate for $10^3 < Re < (2 \times 10^5)$ and $15 \text{ m/s} < u_g < 150 \text{ m/s}$. While a straight forward comparison is not easy, the difference between the value for f_{pg} as predicted by Eq. 14 versus that by Eq. 16 can be seen in the example. At $Re = 10^4$ and $\phi = 0.4$, Eq. 14 gives $f_{pg} = 53{,}000$ and Eq. 16 gives a value of $f_{pg} = 5448$. To utilize Eq. 16 one must specify the average gas velocity, u_g, and the particle radius, r_p, that were used to obtain the Reynolds number. A kinematic viscosity $\mu_g/\rho_g = 1.8 \times 10^{-6}$ m^2/sec, a particle radius $r_p = 1.0$ mm, and an average gas velocity $u_g = 30.5$ m/sec were used to obtain a Reynolds number $Re \cong 10^4$. From this

*Data from Ref. 10 was limited to $u_g < 300$ m/sec.

particular example, the Wilcox/Krier correlation (Eq. 16) allows about 10 times the permeability, i.e., 1/10 the viscous drag force as correlated by the Kuo/Nydegger relation.

Solutions to the flow process leading to DDT, discussed in the following chapter, clearly indicate that sufficient gas permeability is necessary to allow for a detonation transition.

NUMERICAL INTEGRATION

Finite Difference Mesh

To solve the Eulerian formulated system of conservation equations discussed above with the constitutive relations listed in Appendix A, the length of the bed being integrated over is divided into I segments, each a constant Δx in width (i.e., $x_j = j\Delta x$; $j = 1, 2, 3....I$).

At time $t = 0$ values of the nine independent variables; ρ_g, ρ_p, u_g, u_p, T_g, T_p. P_g, P_p and ϕ are initialized at each jth x-location in the grid. Before incrementing the primary variables (i.e. mass, momentum and energy) to the future time, $t = t_o + \Delta t$, the auxiliary variables in the equations (e.g., drag, gas generation, heat transfer) must be computed at the present time, $t = t_o$. The nine equations are then solved at the incremental time, $t = t_o + \Delta t$, by a modified Lax-Wendroff finite differencing scheme. This method, along with another used, are presented in Ref. 5. The second method, developed by Rubin and Berstein [16], was implemented for several test cases and gave results similar to that of the Lax-Wendroff scheme.

The time increment, Δt, over which the equations are solved is calculated by the Courant, Fredrichs, Levy stability criteria, for hyperbolic equations, i.e.,

$$\Delta t = \frac{\lambda \Delta x}{(\underline{c} + |u|)} \tag{17}$$

In Eq. 17 the term $\underline{c}$ is the mixture sound speed and $|u|$ is the maximum gas velocity in the bed. Also, λ is a stability constant, less than unity. For most cases $\lambda = 0.5$ was used. This smaller time increment was necessary in order to integrate the equations when large gradients developed in the flow.

Initial and Boundary Conditions

To initialize the problem the bed is assumed to be quiescent, i.e., at a constant gas temperature and constant gas pressure throughout the length of the bed. The spherical propellant particles are typically fixed at a constant solids loadings, although a variable initial porosity can be treated. Then to initiate the flow, the propellant at the first few grid points is assumed ignited and generating gas. To be consistent with the flat initial pressure profile, all gas and particle velocities at time t = 0 are set equal to zero. Table 1 is a summary of typical input data for the cases studied.

Modification to the Integration Scheme

To solve the flow on a digital computer (which is to represent a DDT phenomena) requires the repetitive integration of many equations. All of the conservation equations and constitutive relations are solved individually at each grid point in the entire bed, for each time increment.

A study of several test cases showed, for instance, that when the ignition front was at a given x-location, there was little activity several grid points ahead of it. That is, the gas and particles were at velocities close to zero and all transport coefficients were negligable in the region not far in front of the ignition front. This phenomena occurred for both the detonation state where the front was propagating between 5-8mm/μsec, and the deflagration state where the propagation velocity was much less. Because of this, an addition was made to the computer code which allows the code to only integrate the active region and bypass the inactive zone.

Ahead of the ignition zone, the computer code located the nearest point to the zone where there was no significant particle or gas movement. This point was then designated as the new front boundary of the integration region for that particular integration step. When the pressure gradient increased, the ignition front moved rather rapidly through the bed (5-10 $\frac{mm}{\mu sec}$) and a new integration boundary had to be located after each time increment.

Comparisons of this modified integration technique with a standard fixed domain integration are reported in Ref. 5 and clearly indicate that the predicted results are almost identical. To assure a correct solution, the actual front integration boundary was extended a few grid points beyond the location calculated by the code. The addition of this new logic to the current code reduced computation time by at least one half, for the same time increment, Δt, and grid space, Δx.

Artificial Smoothing

Inherent to the solution of the system of interdependent conservation equations is a numerical instability. A small perturbation can in some cases amplify with each time increment and eventually destroy the numerical solution. This phenomena can start at the first time increment and in ten to twenty integrations the oscillations can be so large that the solution becomes unstable and terminates. In order to smooth out these oscillations before they amplify, an artificial smoothing routine was incorporated into the code.

From experience in integrating the two-phase flow equations (Eqs. 1-6) with significant nonlinear source-sink terms, the problem of numerical instability occurs often enough to warrant artifical smoothing.

The analyzation of numerous test cases has shown, suprisingly, that the stable solution did not require smoothing of all the variables. It

is obvious that the following results have an inherent dependency on smoothing. Extreme care has been taken to minimize these effects on the qualitative trends and quantitative results predicted. Nevertheless, it should be obvious that smoothing techniques can supply variability in the predicted parameters which are reflections of the scheme utilized, and not necessarily of the conservation equations.

RESULTS COMPUTED

Introduction

This section will present the calculations made for possible DDT occurring in packed beds of high energy, granulated, unisized propellants or explosives. It is obvious that there are a very large number of loading combinations possible for our DDT study. Fortunately, the work of Hoffman and Krier [3] and Krier and Gokhale [2], in which conditions of rapid convective flame spreading have been calculated, is available and can be used as a starting point. (It should be noted that none of the calculations made in Ref. 5, 2 or 3 predicted DDT). As pointed out before, there are probable reasons why this has not been accomplished and it is expected that those improvements and modifications discussed in the previous section will now allow for the calculation of the steady state detonation solution.

The study made of a potential DDT attempts to model a long column of granulated material in a closed pipe ignited by an energetic ignition material at one end. In order to model the flow transient, one must assure that the length of the bed exceeds ℓ_{CJ}, the run-up length to detonation. Since the experimental work of Bernecker and Price [6] indicated that a 10 in (25 cm) bed was sufficient for most of their experiments where DDT occurred, this length was included as a condition to be treated.

Since unisized spheres are being treated, the initial porosity can be no less than $\phi_o = 0.26$, although randomly packed unisized spheres generally give a high porosity, about $\phi_o = 0.40$. Therefore, for this study $0.26 \leq \phi_o \leq 0.40$. The initial particle radii studied were also in the same range as those considered by Refs. 2 and 3. Results in these

studies showed that particles must be less than one millimeter in diameter in order to generate sufficient gases for the rapid flame spreading phenomena.

The chemical energy of the material considered is in the range of explosives or high energy propellants of the nitramine family (i.e., HMX, RDX). Thus, the chemical energies studied were always larger than 4.15 MJ/kg (1000 cal/g). Other parameters one must consider in the DDT studies are the burning rate properties of the propellant. Again, the values used in Refs. 2 and 3, which attempted to model the burning rate of an HMX solid propellant, were utilized. However, the burning rate index, n, is a parameter which is explicitly studied.

In this analysis, the deflagration will be initiated by assuming at time, t = 0, that except for a small portion of the bed at one closed end, the bed is quiescent and unreacting. A closed end situation is always considered, and hence at the two end points (x = 0, x = L) it is assumed that all flow gradients are zero and that the velocities of the particles and gas must also be zero.

The following section presents a solution that indicates (for the first time) a steady state detonation can be predicted. This result is then compared to conditions where no such detonation solution occurs. Additional calculations will indicate the sensitivity of the initial porosity, ϕ_o, chemical energy, E_{CHEM}, burning rate index, n, and ignition energy, E_{ign}, on the run-up length to detonation.

Calculations

Figures 2a and 2b present a case where a transition from deflagration to detonation has occurred. For this example, the burning rate index was n = 1.0, the chemical energy E_{CHEM} = 5.48 MJ/kg and the particle radius

r_p = 127 μm (.005 in).

The pressure-distance profiles at five separate times after ignition of the propellant at x = 0 are shown in Figure 2a. Examining the profile for t = 50 μsec, one can observe that the profile is characterized by a shock front at x = 23 cm followed by a smooth expansion back to the wall at x = 0 cm. The pressure in front of the shock is at atmospheric conditions and, therefore, negligible with respect to the pressure behind the shock.

The ignition locus plot for this particular case is shown in Figure 2b. Here, the ignition front moves through the bed at a low subsonic velocity for the initial ten microseconds and then accelerates to reach a steady state velocity of D_{CJ} = 7.2 mm/μsec. This occurs within 12 to 15 cm from the ignited end. These detonation solutions for P_{CJ} and D_{CJ} are in fair agreement with the approximations of Eqs. 11 and 12 for the given input (E_{CHEM}, ρ_o, γ_j).

Obviously, hydrodynamic steady state analysis (like Eqs. 11 and 12) cannot guarantee that a transition from deflagration to detonation will occur. However, it seems that "critical" values of porosity (related to gas confinement), gas generation rates, and chemical energy will provide for a DDT. For example, when the burning rate index was lowered to n = 0.8, as shown in Figures 3a and 3b, the steep pressure front associated with a detonation did not develop. Correspondingly, no detonation speed was predicted. In this example the peak pressure in the bed never exceeded 5 GPa, no shock was predicted, and only a steady convection-driven front of 2.2 mm/μsec occurred at 100 μsec after ignition of x = 0.

According to Eq. 11, for the case where a transition to detonation actually occurs, the steady state detonation pressure, P_{CJ}, should increase linearly with the chemical energy, E_{CHEM}. Also, Eq. 12 states that the

detonation velocity, D_{CJ}, is a function of the square-root of the chemical energy. Figures 4a and 4b present the results of a calculation where all parameters were identical to those used to give the DDT results of Figures 2a and 2b, except E_{CHEM} = 6.85 MJ/kg, an increase of 25%. The steady state shock pressure predicted for this case, shown in Figure 4a was 21 GPa. This represents a (21/16.4 = 1.28) 28% increase in pressure over the first case. The predicted detonation speed (Fig. 4b), calculated from the slope of the x-t diagram, was 8.70 mm/μsec. According to Eq. 12, the ratio of D_{CJ} for the case given in Figure 4b to that presented in Figure 2b should be

$$\sqrt{(6.85/5.48)} = 1.12$$

This is approximately the increase predicted.

Table 2 summarizes the detonation pressure, P_{CJ}, and the detonation velocity, D_{CJ}, (which were the end results of the DDT calculations) all as a function of the propellant chemical energy. These predicted conditions are compared with the approximate steady state hydrodynamic solutions discussed earlier, i.e., Eqs. 11 and 12. The excellent agreement of the detonation pressure with the analytic solution should be noted.

However, the predicted value for the detonation velocity, D_{CJ}, from the hydrodynamic solution (Eq. 12) shows to be slightly less than the value predicted by the code for all cases. Although one cannot judge which of the two values, detonation velocity or detonation pressure, is more accurate, the percent increase in the detonation velocity as the chemical energy is increased compares favorably with the hydrodynamic solution.

DDT Run-up Length

The run-up length to detonation is defined in this report to be the distance from the closed end where the bed is ignited to the location where both the peak pressure and the detonation speed are constant, i.e., the equilibrium steady state solution.

Figures 5 and 6 plot the predicted run-up length to detonation as a function of the burning rate pressure-index, n (Fig. 5), and initial bed porosity, ϕ_o, (Fig. 6). The "no-solution" boundary indicates that, with the integration scheme used, the mesh size would have had to be drastically reduced (thereby decreasing the integration time increment) in order to obtain a stable solution. This is a costly exercise, but future work is planned to increase the solution regions. Figure 5 clearly indicates that, as expected, one cannot achieve detonation if the burning rate during the deflagration phase is not sufficiently large (see "no transition" boundary). For the solids loading considered ($1-\phi_o = 0.70$), it would appear that a minimum DDT run-up length is 5 cm for particles of 250 μm in diameter.

Figure 6 begins to resemble the required "U-shaped" curve of ℓ_{CJ} versus initial porosity. DDT experiments by Korotkov et.al.[18] show a similar behavior. One would expect that for a relatively porous bed, $\phi_o > 0.60$, no transition will occur since local pressure confinement is limited. If the porosity is too small no gas penetration for the accelerating deflagration wave will occur. The net result is a porosity where a minimum run-up length occurs.

Figure 7 presents a study on the effect of the chemical energy, E_{CHEM}, on the run-up length, ℓ_{CJ}, the values which were presented in Table 2. As expected, the run-up length to detonation increases as the amount of

chemical energy decreases. Again, as expected there is a minimum value where no transition occurs, here about E_{CHEM} = 3.0 MJ/kg. For this case it does appear that a constant but small run-up distance is still required as the chemical energy increases beyond the values studied here.

Detonation Reaction Zone

One measure of the fact that detonation occurs is a plot of the reaction zone width versus the locus of the ignition front. This is presented in Figure 8 where the reaction zone is defined as the region where particles are ignited and generating gas (i.e., $r_p > 0$). As shown, the zone initially increases during the deflagration phase as the convective heat transfer provides energy to ignite more and more of the bed. The zone then collapses to a thin (constant) width as the surrounding high gas pressure causes the particles to burn-out rapidly. A steady reaction zone thickness of approximately 9 mm is predicted.

However, most of the gas is generated in a small region immediately behind the ignition front where the particles are still relatively large. Note that in all the cases reported here, the initial particle diameter was 250 μm. Obviously, initially smaller particles will provide for a thinner detonation reaction zone.

Comments and Interpretations

The results shown in Figures 2-8 have clearly indicated that, as expected, high solids loading of relatively small particle size energetic propellant with confinement will transit into a detonation in space domains of several centimeters. One would expect that propellant properties and packing configurations have limits where detonation cannot occur and this was clearly shown in some of the figures which show the run-up length versus property parameters. In conclusion, it will be useful

to review these studies to determine the properties and configurations which minimize a DDT hazard.

For example, for a fixed chemical energy, E_{CHEM} = 5.48 MJ/kg, a fixed ignition energy, ΔE_{ign} = 9.0 KJ/kg, a fixed particle radius, r_{p_o} = 127 μm (0.005 in) and a fixed solids loading, $(1-\phi_o)$ = 0.7, the burning rate index, n, must be larger than n = 0.86 if DDT is to occur. This was shown in Figure 5. Of course, had the burning rate coefficient, b, been a different number, this exponent may have been different. A general statement can then be made that the burning rate, and hence rate of gas generation, should be kept as low as possible to minimize DDT. Conversely, the higher the burning rate, the better the chance of a transition to detonation occurring.

Figure 6 showed the run-up length to detonation versus initial porosity, ϕ_o. As stated, for all parameters equal, there is a maximum initial porosity where no transition occurs. Since a randomly packed bed of unisized particles has an initial porosity of the order ϕ_o = 0.4, this figure indicates that this is in the region where DDT potential is at a maximum. As one reduces the initial porosity (that is increases the solids loading) the run-up length to detonation slightly decreases until, as experimental work of Bernecker and Price [6] has indicated, there is a minimum initial porosity where DDT cannot occur. Since at these initial solids loadings multi-sized particles and mechanical packing are required, these loadings are not of interest, whereas the randomly packed loadings are of interest.

A similar comparison of the run-up length to detonation was shown in Fig. 7 where the chemical energy content was varied. Recall that a chemical energy, E_{CHEM} = 4.18 MJ/kg (1000 cal/g), can be considered an energetic propellant material. Based on the results shown in Fig. 7, one can

state that less energetic material than this has little chance of encountering a DDT. Doubling the chemical energy from $E_{CHEM} = 4.18$ MJ/kg to $E_{CHEM} = 8.36$ MJ/kg, represents a reduction in the run-up length of only about one half. To summarize, high energy propellant of the nitramine family, where $E_{CHEM} \geq 4.18$ MJ/kg, definitely fall within the regime of a DDT hazard if properly confined.

The final comparison of this type is shown in Figure 9. This shows the run-up length to detonation versus the particle radius. As one would expect, there is a maximum particle radius (i.e., surface-to-volume ratio) where transition is not predicted to occur. This is indicated by the "no-transition" boundary on that figure. The figure also indicates that as the particles get smaller in size, the run-up length to detonation also decreases, as expected. Reducing the initial particle size, r_{p_o}, to values less than 25 μm results in gas generation rates, per unit-volume, that are so large finer grid spacing must be utilized to assure stability. This expensive task has been delayed and is recommended only after improved numerical integration schemes have been developed.

A final topic studied dealt with the effect of ignition temperature (or more appropriately ΔE_{ign}) on the run-up length to detonation. For the results shown in this chapter a nominal value of $T_{ign} = 303°K$ was used. For this study $\phi_o = 0.30$, $r_{po} = 127$ μm and $n = 1.0$.

Calculations were made in which T_{ign} varied over the range $294°K < T_{ign} \leq 350°K$. For a constant initial bed temperature of $T_{g_o} = T_{p_o} = 294°K$ this represents a range of ignition energy of $0.0 < \Delta E_{ign} \leq 25.7 \frac{KJ.}{kg}$

For most of the ignition temperatures tested there was little change in the steady state detonation pressure or velocity. Only when ΔE_{ign} approached the improbable value of $\Delta E_{ign} \to 0$ did the values change significantly.

REFERENCES

1. Van Tassel, W.F. and Krier, H., "Combustion and Flame Spreading Phenomena in Gas-Permeable Explosive Materials," International Journal of Heat and Mass Transfer 18, 1377-1386 (1975).

2. Krier, H. and Gokhale, S.S., "Modeling of Convective Mode Combustion Through Granulated Propellant to Predict Detonation Transition," AIAA Journal 16 (2), 177 (1978).

3. Hoffman, S.J. and Krier, H., "Fluid Mechanical Processes of Deflagration to Detonation Transition in Beds of Porous Reactive Solids," Technical Report AAE 80-2, UIUL-ENG 80-502, Aeronautical and Astronautical Engineering Department, University of Illinois at Urbana-Champaign, IL 1980.

4. Krier, H., and Kezerle, J.A., "A Separated Two-Phase Flow Analysis to Study Deflagration-to-Detonation Transition (DDT) in Granulated Propellant," Seventeenth Symposium (International) on Combustion, The Combustion Institute, Pittsburgh, PA 1979.

5. Butler, P.B. and Krier. H., Technical Report AAE 81-1, UILU-ENG 81 0501, Aeronautical and Astronautical Engineering Department, University of Illinois at Urbana-Champaign, IL 1981.

6. Bernecker, R.R. and Price, D., "Studies in the Transition from Deflagration to Detonation in Granular Explosives - I Experimental Arrangement and Behavior of Explosives which Fail to Exhibit Detonation," Combustion and Flame 22, 111 (1974).

7. Bernecker, R.R. and Price, D., "Studies in the Transition from Deflagration to Detonation in Granular Explosives - II Transitional Characteristics and Mechanisms Observed in 91/9 RDX/Wax," Combustion and Flame 22, 119 (1974).

8. Griffiths, N. and Groocock, J. M., "The Burning to Detonation of Solid Explosives," Journal of Chemical Society, p. 4154 (1960).

9. Taylor, J. W., Trans. Faraday Soc. 58, 561 (1962).

10. Wilcox, S. F. and Krier, H., Technical Report UILU-ENG 80-0501, University of Illinois at Urbana-Champaign (March 1980).

11. Jacobs, S. J., private communication with H. Krier and S. S. Gokhale, White Oak Laboratory, Silver Springs, MD, March 1978.

12. Cook, M. A., "An Equation of State for Gases at Extremely High Pressures and Temperatures from the Hydrodynamic Theory of Detonations," The Journal of Chemical Physics 15 (7) (1947).

13. Kamlet, M. J. and Jacobs, S. J., "Chemistry of Detonations - I - A Simple Method for Calculating Detonation Properties of C-H-N-O Explosives," Journal of Chemical Physics, 48, pp. 23-25 (1968).

14. Kuo, K. K. and Nydegger, C. C., Journal of Ballistics, 2 (1), pp. 1-25 (1978).

15. Rubin, E. L. and Berstein, S. Z., "Difference Methods for the Inviscid and Viscous Equations of a Compressible Gas," Journal of Computational Physics, 2, 178-196 (1967).

16. Lembeck, M. F., Butler, P. B., and Krier, H., "Smoothing Techniques to Solve Shock Formation in Two-Phase Flows," University of Illinois at Urbana-Champaign, in press (1981).

17. Korotkov, A. I., Sulimov, A. A., Obmenin, A. V., Dubovitskii, V. F. and Kurkin, A. I., "Transition from Combustion to Detonation in Porous Explosives," Fizika Goreniya i Vzryva, 5, 315 (1969).

TABLE 1

Typical Input Data

PARAMETER	VALUE
Burning Rate Index	$0.8 < n < 1.2$
Burning Rate Proportionality Constant	$b = 0.001 \frac{in}{sec} [\frac{1}{PSI}]^n$
Initial Bed Porosity	$0.25 \leq \phi_o \leq 0.50$
Particle Diameter	$50\mu m \leq d_p \leq 500\mu m$
Bed Length	$L = 25.0$ cm
Grid Spacing	$\Delta x = 1.27$ mm
Chemical Energy	$4 \frac{MJ}{kg} < E_{CHEM} < 7 \frac{MJ}{kg}$
Gas Specific Heat	$1.0 \frac{KJ}{kg°k} \leq C_{vg} \leq 1.9 \frac{KJ}{kg°k}$
Initial Bed Temperature	$T_g = 294°K$
Ignition Temperature (Bulk)	$T_{ign} = 303°K$
Ignition Energy	$E_{ign} = 9.0 \frac{KJ}{kg}$

TABLE 2

Comparison of the Predicted Detonation State with

an Approximate Hydrodynamic Solution

E_{CHEM}	P_{CJ}(predicted)	P_{CJ}(Eq. 11)*	D_{CJ}(predicted)	D_{CJ}(Eq. 12)**	ℓ_{CJ}
4.11 MJ/kg	14.0 GPa	12.0 GPa	6.48 $\frac{mm}{\mu sec}$	5.12 $\frac{mm}{\mu sec}$	89 mm
5.48	16.6	16.07	7.25	5.92	51
6.85	21.8	20.08	8.24	6.62	44
8.22	24.6	24.1	9.17	7.25	38
10.96	30.0	33.2	10.58	8.37	28

* $P_{CJ} = 2(\gamma_J - 1)\ \rho_p(1-\phi)\ E_{CHEM}$ (Eq. 11)

** $D_{CJ}^2 = 2(\gamma_J^2 - 1)\ E_{CHEM}$ (Eq. 12)

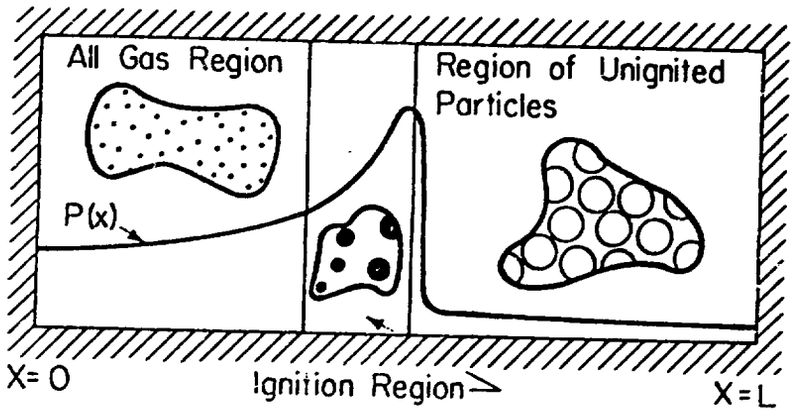

Fig. 1. Schematic of packed bed after transition to detonation. Ignition region has collapsed to a thin zone and is followed by an all gas region (not to scale).

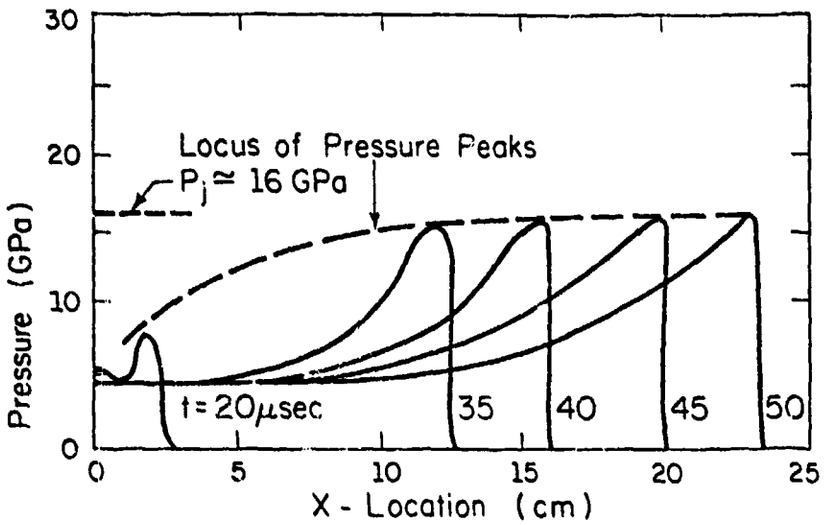

Fig. 2a. Pressure history during accelerating deflagration in a packed bed leading to a detonation transition (n = 1.0)

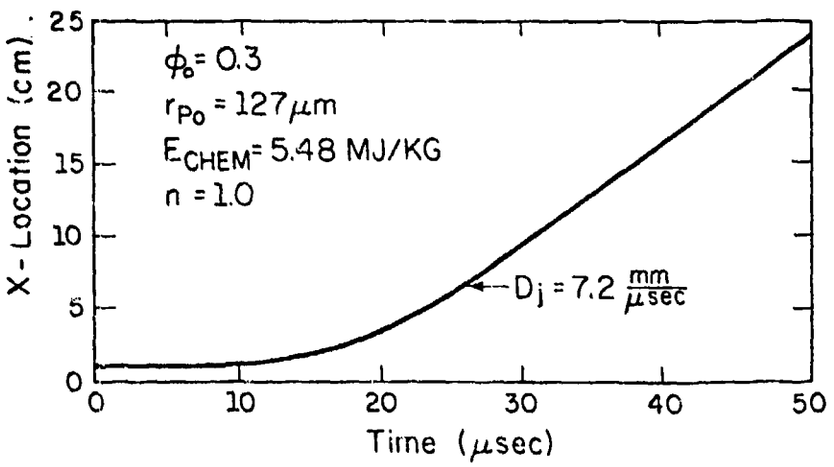

Fig. 2b. Ignition front locus with detonation transition (n = 1.0)

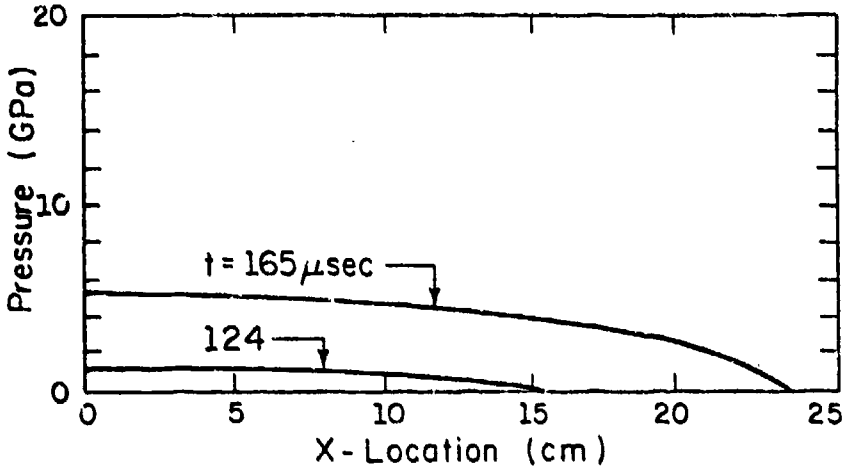

Fig. 3a. Pressure history during deflagration with no transition (n = 0.8).

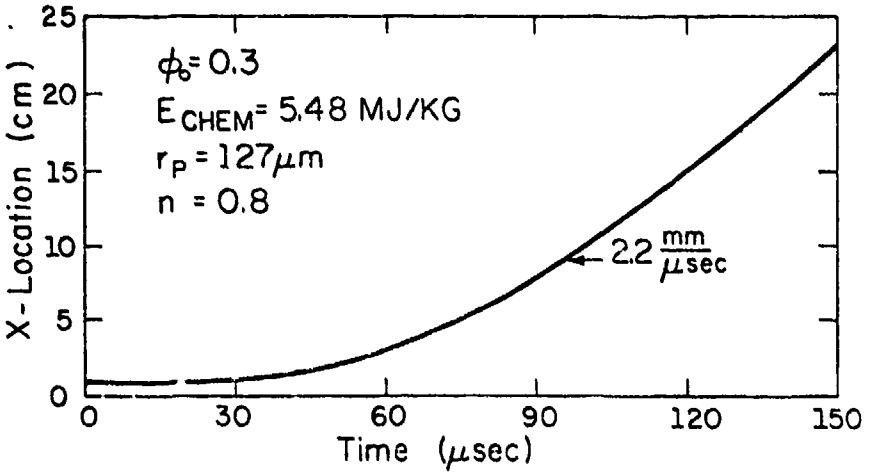

Fig. 3b. Ignition front locus with no detonation (n = 0.8).

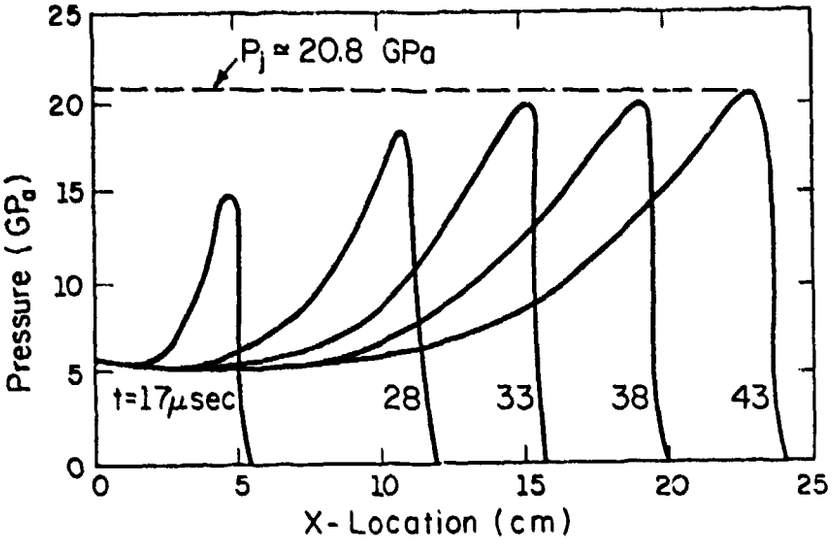

Fig. 4a. Pressure history leading to detonation with 25% increase in E_{CHEM} (compare to case shown in Fig. 2a).

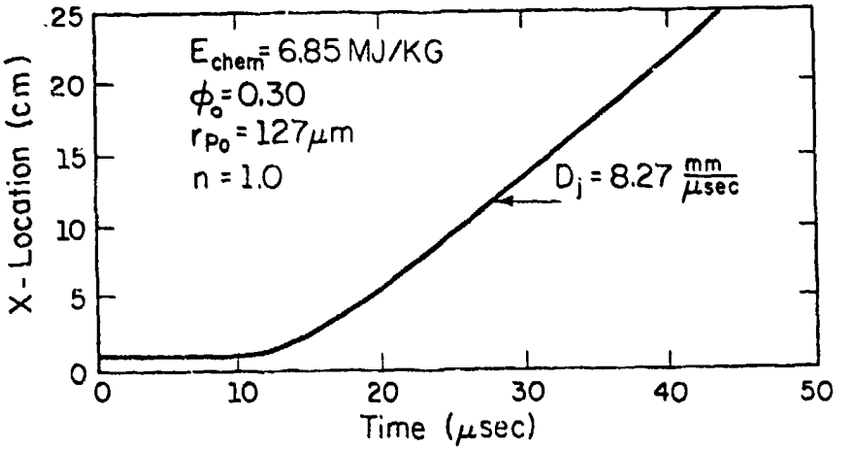

Fig. 4b. Ignition front locus (compare to Fig. 2b)

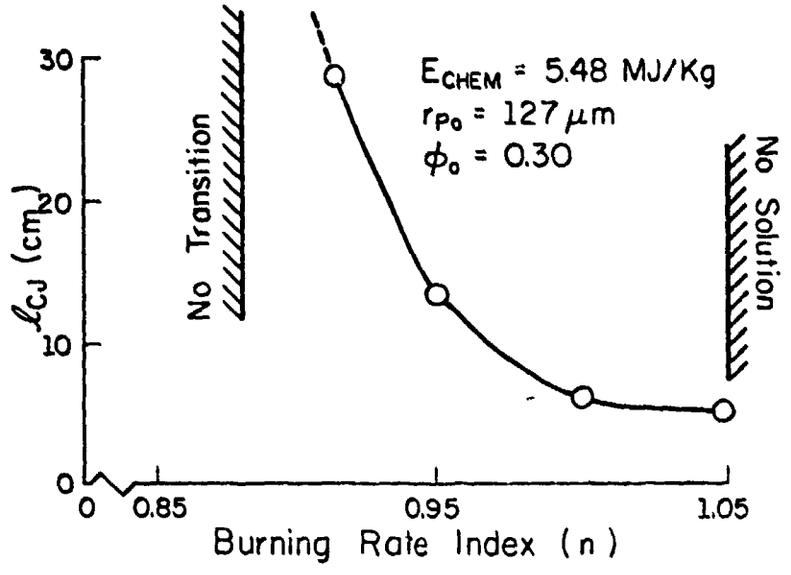

Fig. 5. Variation in burning rate pressure index, n, on run-up length, ℓ_{CJ}.

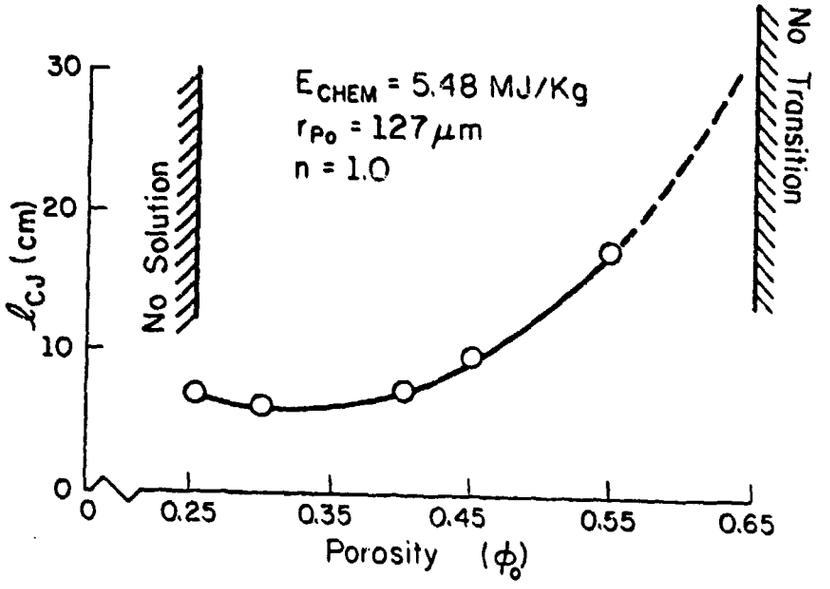

Fig. 6. Variation in initial bed porosity, ϕ_o, on run-up length, ℓ_{CJ}.

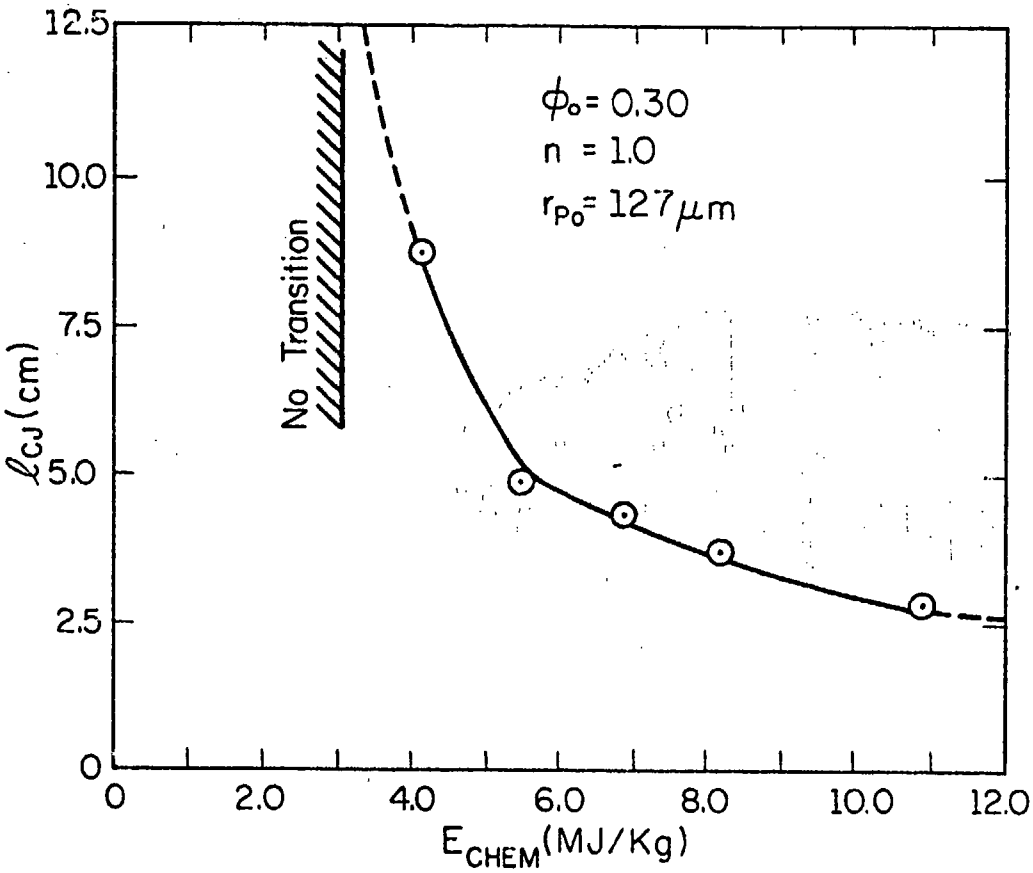

Fig. 7. Variation in run-up length to detonation, $\ell_{C.J}$, with chemical energy, E_{CHEM}.

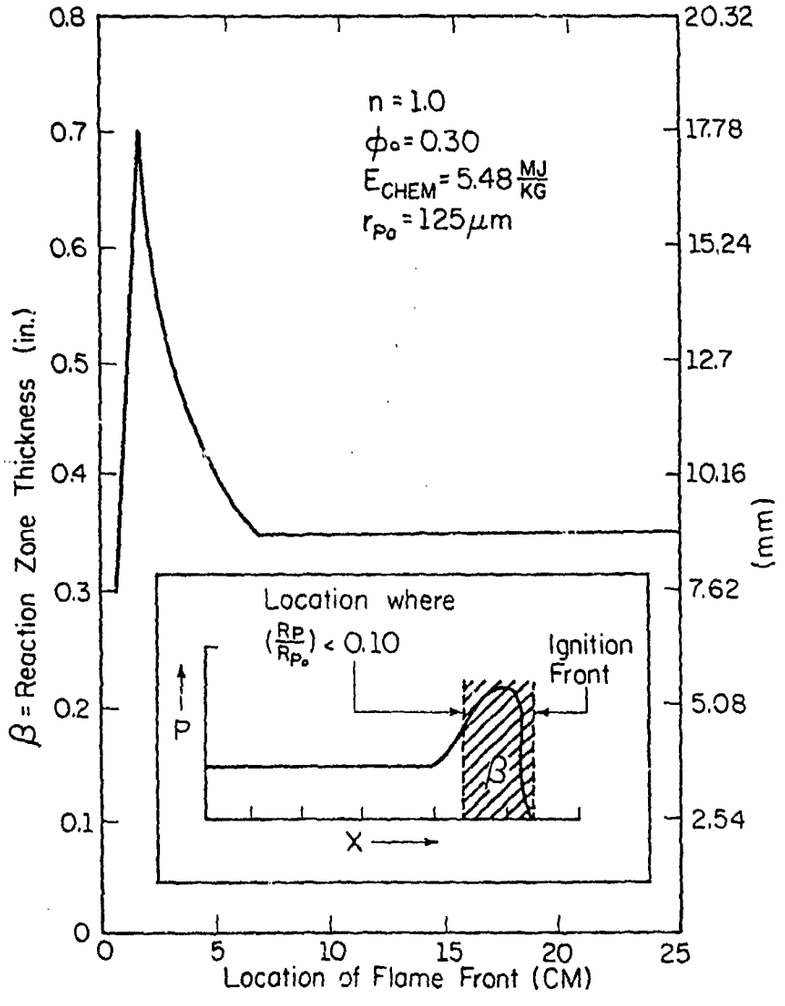

Fig. 8. Reaction (propellant gasification) zone thickness during an accelerating deflagration leading to a detonation.

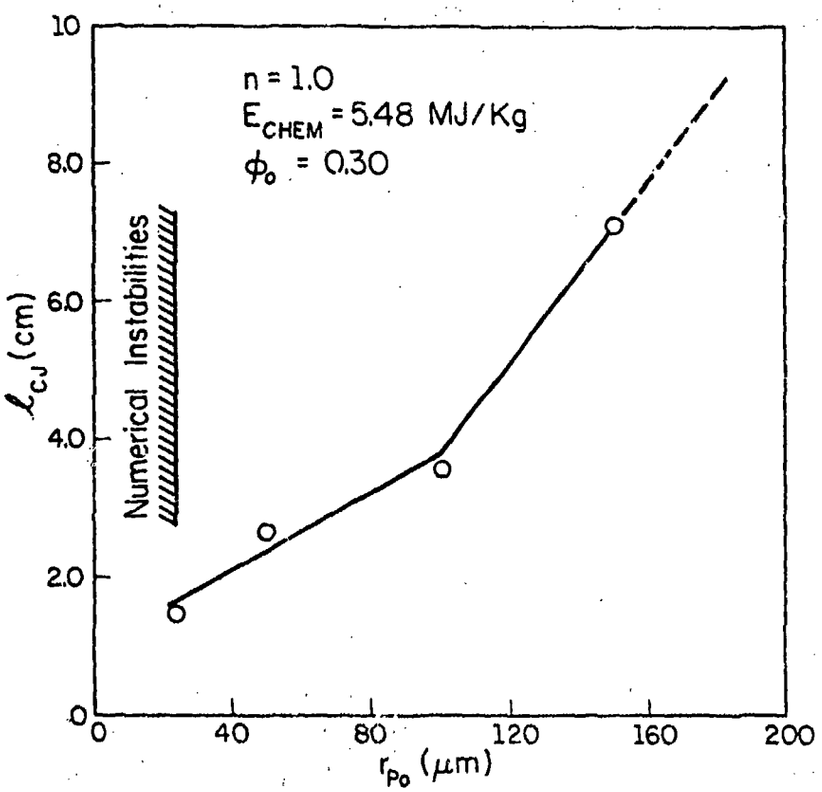

Fig. 9. Run-up length to detonation versus initial particle radius, r_{p_o}.

APPENDIX A

CONSTITUTIVE RELATIONS

As discussed earlier, a system of nine independent equations is necessary in order to solve for the nine unknown variables describing two-phase flow: ρ_g, ρ_p, u_g, u_p, E_g, E_p, P_g, P_p and ϕ.

Of the three additional equations necessary for the solution, one is the ninideal equation of state for the gas phase as described in the text.

$$\frac{P_g}{RT_g} = 1 + b\rho_g + c\ (b\rho_g)^2 + \ldots \qquad (A.1)$$

Values for the constants b and c are discussed in Ref. 5.

The second represents an equation of state which relates the solid density to the stress on the particle. (See Ref. 3).

$$P_p = \left(\left(\frac{\rho_p}{\rho_{p_o}}\right)^3 - 1\right) \frac{K_o}{3} \qquad (A.2)$$

Finally, the third additional constraint is a relation for the particle phase stress, P_p, as a function of the solids loading and the material bulk modulus, K_o (also see Ref. 3).

As discussed in References 2 and 3, one must also specify functional relations for the following:

a) $\Gamma \equiv$ mass generation rate per unit volume

$$\Gamma = \frac{3}{r_p} (1-\phi)\ \rho_p\ \dot{r} \qquad (A.3)$$

Here, r_p is the instantaneous particle radius and $\dot{r}$ is the surface burning rate specified as a function of pressure (and possibly particle temperature).

For all cases run in this study:

$$\dot{r} = \underline{b} p^{n} \tag{A.4}$$

where $\dot{r}$ has units of (in/sec), P (psi) and $\underline{b}$ is of the order $(1 \times 10^{3}) \frac{\text{in/sec}}{(\text{psi})^{n}}$.

b) $\mathcal{D} \equiv$ interphase (gas-particle) viscous force (as discussed in the text).

$$\mathcal{D} = \frac{\mu_g}{4 r_p^{2}} (u_g - u_p) f_{pg} \tag{A.5}$$

where

$$f_{pg} = 5.06 \times 10^{5} r_p \, Re/u_g^{2}$$

c) $\dot{Q} \equiv$ interphase heat transfer rate

$$\dot{Q} = \frac{3}{r_p} (1-\phi) h_{pg} (T_g - T_p) \tag{A.6}$$

In the analysis carried out here, the heat transfer coefficient was

$$h_{pg} = 0.65 \left[\frac{k_g}{2 r_p}\right] [Re]^{0.7} (Pr)^{0.33} \tag{A.7}$$

where k_g is the thermal conductivity, Re is the Reynolds number and Pr is the Prandtl number.

Roger A. Strehlow

Accidental Explosions

Recent research has significantly increased our understanding of the causes and behavior of accidental explosions and has produced new and more effective safety measures

Accidental explosions are an undesirable side effect of man's technological development. The first such explosions were undoubtedly associated with the manufacture, handling, and use of black powder. In the Middle Ages alchemists inadvertently caused explosions by mixing incompatible chemicals. The development by Lavoisier (1789) of a systematic nomenclature for inorganic compounds led to the golden age of preparative chemistry, during which many new explosive substances and mixtures were prepared, resulting in more laboratory-scale explosions. This in turn led quickly to larger accidental explosions with the development of the new field of high explosive technology.

At about the same time, the industrial revolution, with its need for fossil fuel energy, introduced coal mine explosions to mankind. The commercialization of grain handling and milling in the nineteenth century led to many major grain elevator and mill explosions (Price and Brown 1922). The recent development of larger and larger single-line petrochemical process units and the bulk transport and storage of ever increasing quantities of fuels under high pressure or at low temperature have led to boiling-liquid expanding-vapor explosions, or BLEVEs, and unconfined vapor-cloud explosions. These can be disastrous, and their frequent incidence in the last decade has led to a resurgence of research into the nature of all explosions.

The term *explosion* is not very precise. I shall use it in this article to mean a process in which the production or release of a gas under high pressure is rapid enough to cause a pressure wave, usually called a blast wave, to propagate through the surrounding medium, usually air. Explosions are audible at some distance from the source: nearby an explosion is heard as a sharp "crack," while far away, owing to atmospheric inhomogeneities, it is heard as a "boom."

The most important aspect of any accidental explosion is of course the damage it produces, and I shall discuss briefly how destruction occurs. Next I shall describe the sequence of events that leads to explosions and the processes in the source region during the explosion itself. Then I shall consider the current status of research on accidental explosions.

Roger A. Strehlow is Professor in the Department of Aeronautical and Astronautical Engineering at the University of Illinois. He received his Ph.D. in physical chemistry from the University of Wisconsin. His research has included reactive gas dynamics, flame propagation, and the initiation and structure of detonation waves; his recent interest focuses on combustion hazards and industrial safety, and he is currently studying lean limit flame extinction and nonideal blast waves. He is at present chairman of a National Research Council panel on the causes and prevention of grain elevator explosions. Address: 105 Transportation Building, University of Illinois, Urbana, IL 61801.

Damage mechanisms

Explosion damage occurs for a number of reasons. The enclosing structure can be blown apart and become the source of primary fragments. The blast wave can inflict damage on objects it encounters, sometimes producing secondary fragments that can damage other objects (e.g. flying glass from windows). Radiation from certain combustion explosions can cause burns and ignite combustible material at a distance.

Internal damage to the enclosing structure, though difficult to quantify, can be used to evaluate the course of an explosion. In buildings the direction in which objects such as walls, partitions, furniture, etc., are displaced can usually be used to diagnose the progress of the explosion. Metal vessels rupture in either a brittle or ductile mode, depending on the particular metal, its temperature, and the rate of application of the internal pressure. In certain cases, analysis of the trajectories of primary fragments can be used to deduce the forces acting at the moment of rupture (U.S. Atomic Energy Commission 1966). Baker and co-workers (1975, 1978) have shown that primary fragment patterns, though somewhat irreproducible, can be predicted with reasonable accuracy.

The blast wave produced by an explosion is called a free-field blast wave until it interacts with objects in its path. Its structure is quite dependent upon the behavior of the source of the explosion. If the source has a very high energy density (units, J m^{-3}) and also a high power density (units, J m^{-3} s^{-1}), i.e. releases the energy very rapidly, both the source and the blast wave are said to be ideal.

Our understanding of the structure, scaling laws, and damage potential of an ideal blast wave is now well developed (Lee et al. 1969; Baker 1973; Swisdak 1975). Three kinds of explosions that yield ideal blast waves are point source explosions, nuclear explosions, and condensed phase detonations. A point source explosion is a mathematical idealization: a fixed amount of energy is released at a point in an infinite uniform atmosphere in an infinitesimal time. Its energy and power densities are therefore infinite. A small volume of

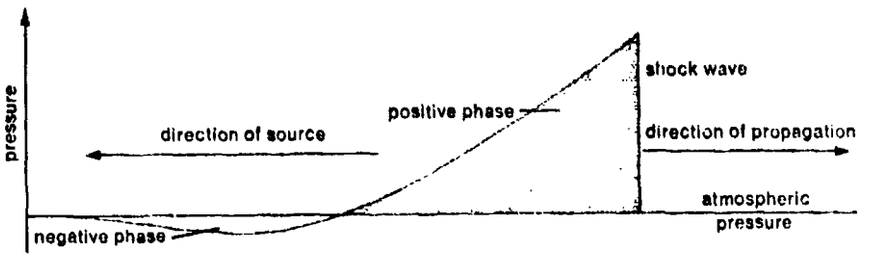

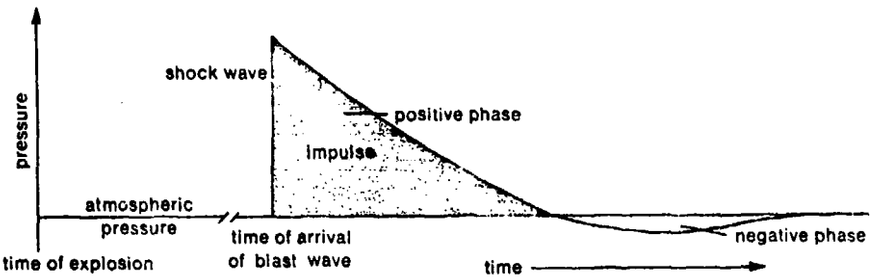

Figure 1. The blast wave from an ideal explosion is a simple pressure wave with spherical symmetry, the leading edge of which is a shock wave. In its wake, the pressure drops to a subatmospheric level (negative phase) before returning to the ambient level due to recompression. The shape of the wave at any instant in time is shown at the top, and the experience of a stationary observer as the blast wave passes is shown at the bottom. (After Baker 1973.)

air in the vicinity of the source is compressed and heated, thereby producing a region of very high pressure that is bounded by a strong spherical shock wave. This wave decays as it travels away from the source and eventually becomes a weak acoustic wave.

Nuclear explosions and condensed phase detonations also have very high energy and power densities. Their blast waves become ideal waves before their shock pressures have dropped below the levels required for total destruction of objects in their paths. Thus, for all practical purposes, their blast waves may be considered ideal, even though there are near-field differences. Sachs (1944) was the first to show that the temporal structure of all ideal blast waves is similar, and that their properties are related only to the total energy of the source and the distance of the observer from the source.

A free-field blast wave interacts with objects it encounters in a very complex manner. The shock is reflected and refracted, and produces higher pressures locally than those measured in the free field, thereby causing objects to bend, buckle, tear, or shatter.

Sperrazza (1951) was the first to show empirically that blast damage *in any specific mode* is related to both the peak overpressure, P, and the positive impulse, I, of the wave (Fig. 1). Specifically he observed that there is an impulse asymptote below which there is no damage, irrespective of the magnitude of the overpressure, and an overpressure asymptote below which there is no damage, irrespective of the impulse (or duration) of the blast loading. An example of this behavior is shown in Figure 2. Newmark (1953) independently and analytically identified the two P-I threshold asymptotes for damage, using the concept of energy absorption. Baker and his colleagues (1978) showed recently that the Jarrett (1968) formula for blast damage to brick houses, which was developed empirically from bomb damage during World War II, yields typical asymptotic behavior when plotted in the P-I plane. This is especially interesting since, unlike Sperrazza, they did not specifically identify impulse as being important.

The response of objects to drag forces induced by the blast wave is more complex than that predicted by simple P-I response curves (Baker et al. 1978). This is because the kinetic energy of the flow associated with the blast wave imposes a drag force which can cause bending of thin objects such

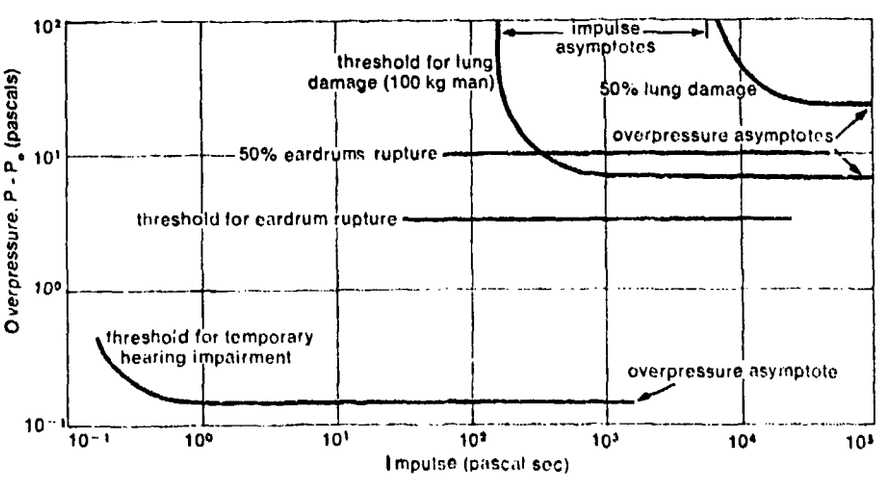

Figure 2. For lung damage in man, both overpressure and impulse asymptotes have been observed. For eardrum rupture, only the overpressure asymptote has been observed. The response of the eardrum is so rapid that even a blast wave with a small impulse appears as a pulse of long duration, making it impossible to observe the impulse asymptote. Even for temporary hearing impairment (~24 hr), it has not been possible to observe the impulse asymptote, even though the curve is rising toward the asymptote. (After Baker et al. 1978.)

as flagpoles or light standards, or tumbling or gross displacement of unattached bodies such as trucks or people (Baker et al. 1973). The drag force is dependent on both the shape of the blast wave and the detailed shape and orientation of the object. Penny and his colleagues (1970) based their determination of the TNT equivalent of the Hiroshima and Nagasaki atomic bombs on such drag forces.

If the accidental explosion is a combustion explosion and produces a fireball, radiation damage can be severe. The amount of radiation is primarily a function of the size and duration of the fireball, since fireball temperatures for most fuels are approximately the same (≈ 1350°K). Recently it has been postulated that fireball damage can be evaluated by a technique similar to the *P-I* technique for blast-wave damage (Baker et al. 1978). In this case the static pressure asymptote is replaced by a radiation flux rate asymptote for long exposures, and the impulse asymptote by an asymptote representing the total flux for exposures of short duration. The approach looks promising and may eventually provide information on the extent of the damage for specific exposure levels and reasonable criteria for allowable fireball exposure.

Types of accidental explosions

The term *accidental explosion* covers a wide spectrum, and obviously no two explosions are exactly alike. It is nevertheless possible to group accidental explosions into nine major categories, each with its own distinctive characteristics (Table 1).

Table 1. Categories of accidental explosions and where they are most likely to occur

Type of explosion	*Typical situations*
Condensed phase detonations	Chemical reactors, distillation columns, separators, factories that produce high explosives and propellants
Combustion explosions of gaseous or liquid fuels in enclosures	Buildings, ships, tankers, boilers, compressed-air lines
Combustion explosions of dusts in enclosures	Coal mines, grain elevators, pharmaceutical industry
Boiling-liquid expanding-vapor explosions (BLEVEs)	Ductile vessels such as tank cars containing combustible high vapor-pressure liquids
Unconfined vapor-cloud explosions	Spills of highly volatile fuels, chemical plants
Explosions of pressurized vessels containing nonreactive gaseous materials	Boilers, pressurized gas tanks
Explosions resulting from chemical reactor runaway	Chemical reactors
Physical vapor explosions	Island volcanoes, molten material poured into a moist container
Explosions resulting from nuclear reactor runaway	Nuclear reactors

Condensed phase detonations approximate ideal explosions—those with infinite energy and power densities—although in practice the blast wave is usually attenuated somewhat due to confinement. Blast and fragment damage can be estimated if the quantity of material and the degree of confinement are known (AMCP 1972; Baker 1973; Swisdak 1975). There have been detonations of this sort during the manufacture, transport, storage, and use of high explosives and propellants, and in chemical reactors, distillation columns, separators, etc., when some unwanted and highly sensitive substance has accidentally been allowed to concentrate.

When large quantities of high explosives are handled or stored in bulk or in containers that are in relatively close contact, detonation can be truly disastrous. In 1921, in Oppau, Germany, a congealed mass of 4.1×10^6 kg of ammonium nitrate-sulfate double salt that was being broken up with dynamite for use as fertilizer detonated as a unit, killing an estimated 1,100 people, causing severe damage up to 6 km away, and leaving a crater 130 m in diameter and 60 m deep. Until the time of the disaster, it had been thought that this salt, even though exothermic, could not support a detonation. Even today, laboratory-scale testing would indicate that it is nondetonatable because its minimum charge diameter for detonation is much larger than the size usually used for sensitivity tests. Another major explosion involving ammonium nitrate took place in Texas City in April 1947, when the ship *Grand Camp* caught fire (Wheaton 1948). The fire accelerated out of control, causing the ammonium nitrate in the hold to detonate. All houses within a 1.5 km radius were totally destroyed, and it was estimated that 516 people were killed and that property damage amounted to $67 million.

The second type of explosion, the *combustion explosion of a gaseous or liquid fuel in an enclosure,* has two distinct limit behaviors. An enclosure that has a length-to-diameter ratio (L/D) of about one and that is not too cluttered with equipment, partitions, etc., will usually suffer a simple overpressure explosion. The rise in pressure is relatively slow, and the weakest windows or walls blow out first. In a simple frame building, the ceiling will rise and the walls will all fall out at about the same time. In a steel container like a ship hold or a boiler, the enclosure will tend to become spherical until a tear or rip vents the contents. Although the damage to the enclosure may be extensive, the resultant blast wave is ordinarily quite weak, because, in general, buildings, ships, or boilers vent at very low overpressures (7–70 kPa or 1–10 psig).

In enclosures that have large L/D ratios or contain large pieces of equip-

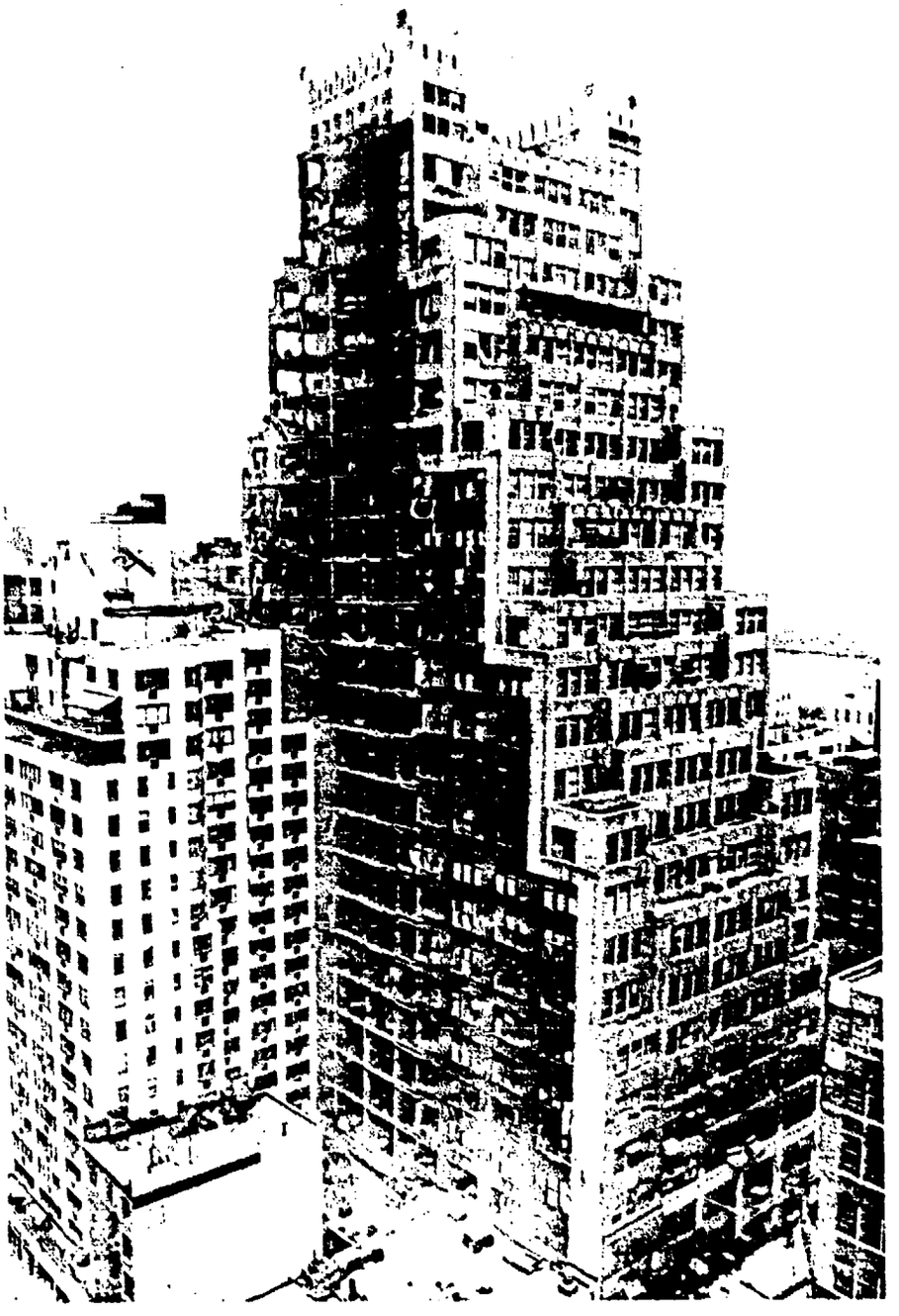

Figure 3. An internal natural gas explosion in the elevator shafts (located on the left-hand face) of a 25-story commercial building blew out all the bricks surrounding the shafts and virtually all the windows. The accident occurred in April 1974 in New York City. (From NTSB 1976.)

ment or internal partitions, flame propagation following ignition causes gas motion ahead of the flame, which generates turbulence and large-scale eddy folding where the flow is interrupted by obstacles. This in turn causes a rapid increase in the effective flame area, resulting in a more rapid rise of pressure and further turbulent/eddy interactions. Local pressures can become very high (≈1.5 mPa or 15 atm) very rapidly (<1/1,000 sec) and can lead to gas-phase detonations with highly localized massive damage. The damage is usually greatest furthest away from the source of ignition. These detonations frequently produce strong blast waves and high-velocity fragments, causing more damage to the surroundings than simple overpressure explosions. Commercial buildings often explode in a manner indicative of significant wave propagation and flame acceleration (Fig. 3). Explosions of this sort also take place in compressed-air lines, where the fuel is oil or char on the walls (Burgoyne and Craven 1973).

Halvorsen (1975) presents examples of tanker explosions, most of which are simple pressure explosions that occur in spaces with low L/D ratios. However, some tanker explosions produce the highly localized damage typical of explosions in high L/D enclosures. Figure 4 shows the remains of such an explosion, caused by external ignition of escaping fuel vapor during ballasting. Many tanker and supertanker explosions are ignited by sparks of static electricity generated by the high pressure water spray used for cleaning.

Combustion explosions of dusts in enclosures can be quite disastrous (Palmer 1973; Bartknecht 1978). Contrary to some commonly held beliefs, virtually all organic dusts, as well as certain inorganic or metallic dusts, are combustible in air and can explode if enclosed. Dust explosions exhibit the same L/D limit behaviors as gas and vapor explosions, but the sequence of events is different. Combustible quantities of airborne dust normally exist only inside ducting or process equipment (e.g. hammer mills, driers, etc.). A small explosion in such equipment causes it to rupture and throw burning dust into the work place. If the work area is dirty, the resulting gas motion and the vibration of equipment cause the layered dust to become airborne and then fuel a more violent second explosion, which travels through the work place causing major damage.

In another typical sequence, a pile of dust starts to smolder either by spontaneous combustion or because it is covering a hot object such as a motor housing or a lamp fixture. A worker finds the fire and attempts to put it out with a chemical extinguisher or a water hose, stirring up a large cloud of dust, a portion of which is already burning, and an explosion results.

Coal mine explosions have been common since the start of the industrial revolution. Most industrial nations have extensive research programs to investigate such explosions, and the dynamics of the explosion

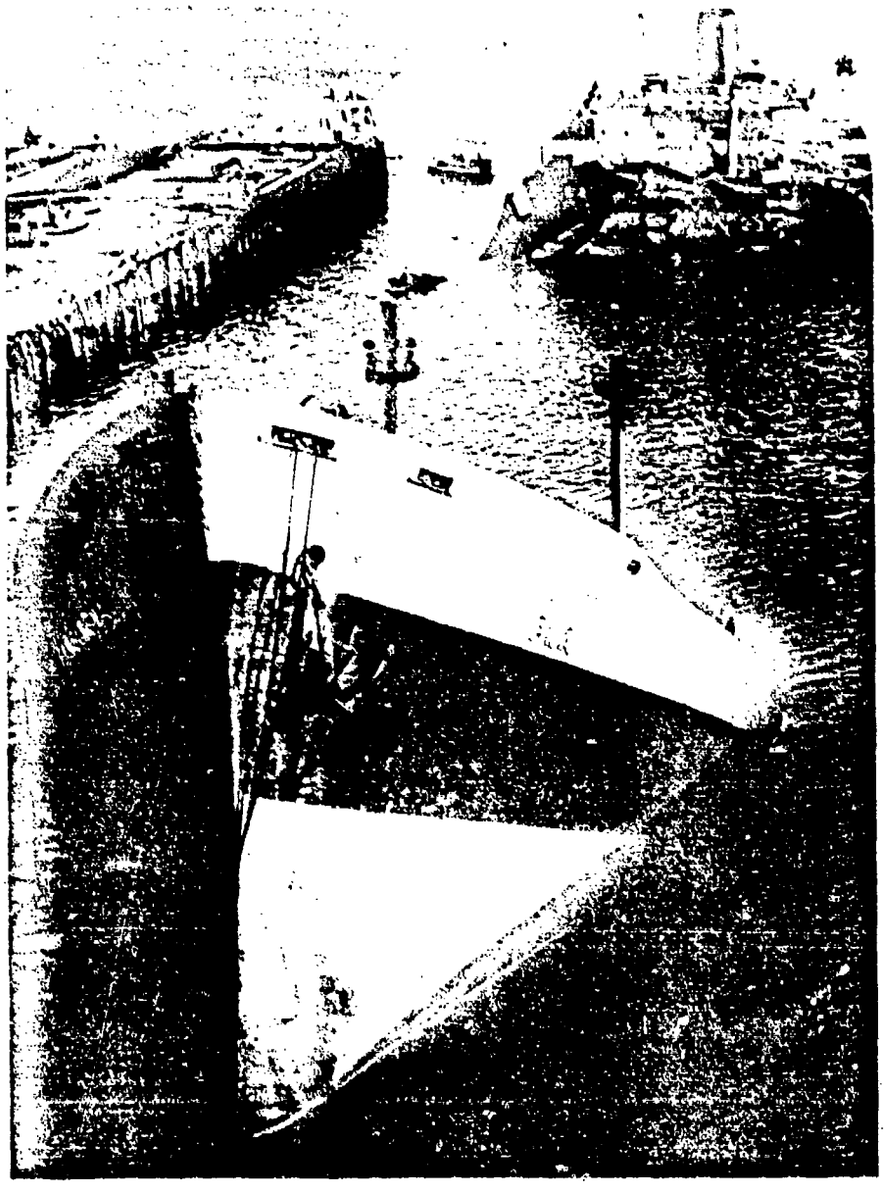

Figure 4. While the Liberian tanker *S.S. Sansinena* (250 m long and 32 m wide) was being ballasted in Los Angeles harbor in December 1976, a cloud of combustible vapor from the hold formed on the deck and was ignited by an unknown source. The resulting flash fire entered the hold, setting off an explosion. Witnesses reported that the entire tank deck and midship deckhouse rose 250 m into the air, leaving only the part shown here. Severe damage was reported up to 2 km away, and windows were broken up to 4 km away. The explosion killed 6, left 3 missing, injured 58, and caused $21.6 million in damage. (From USCG 1977.)

process are reasonably well understood. Ignition is usually effected by the release and ignition of a pocket of methane in the mine, or by detonation of the explosives used in blasting. Since a mine is always quite dirty, because it is expensive to remove all the coal dust, the resulting dust explosion propagates over long distances. Although the annual number of deaths from coal mine explosions in the United States has decreased by more than half since the beginning of the century (Cybalski 1975), mine explosions will undoubtedly occur in the future.

Dust explosions in grain elevators and in various milling industries are also common, averaging ten to fifteen a year in the United States. In December 1977 two disastrous explosions took place within five days of each other, at the Continental grain facility in Westwego, LA, and at the Farmers Export grain elevator in Galveston, TX, significantly reducing the grain-exporting capacity of the United States.

Boiling-liquid expanding-vapor explosions, or BLEVEs, occur when a ductile vessel containing a liquid with a vapor pressure well above atmospheric pressure tears open. In these explosions the tearing process is relatively slow, and a small number of large fragments are produced. Because they are backed by a liquid that can evaporate very rapidly (flash evaporate), even large fragments can be thrown up to 700 m. If the liquid in the tank is combustible and the BLEVE is caused by heat from an external fire, a buoyant fireball is produced, the duration and size of which are determined by the total weight of fluid enclosed in the tank. The BLEVE of a standard 33,000 gallon tank car containing a flash-evaporating fuel such as liquid petroleum gas will create a fireball, the radius of which is ~50 m at ground level and ~100 m once it becomes airborne. Thus, even when the blast damage is mild, missile and fireball damage can be catastrophic.

In an *unconfined vapor-cloud explosion*, the first event is the massive spill of a combustible hydrocarbon into the atmosphere. Following this, one of four things can happen: the spill may be dissipated harmlessly without ignition; it may be ignited immediately upon release, causing a fire but no explosion; it may be dispersed over a wide area before being ignited, causing a large fire; or, if the flame accelerates rapidly enough, a dangerous blast wave can be produced (Strehlow 1973).

Unconfined vapor-cloud explosions can be both very spectacular and very dangerous, because the leak is into the open air, and, with the right meteorological conditions, extremely large clouds of the combustible mixture can be produced before ignition occurs. In June 1974 at the Nypro

chemical plant near Flixborough, England, approximately 45,000 kg of cyclohexanone at a pressure of 850 kPa (125 psig) and a temperature of 155°C was released through two 0.7 m diameter stub pipes and flash-evaporated, producing a sizable cloud throughout the plant. Ignition probably occurred at a furnace in the hydrogen plant some distance from the release point, and the fire was already large by the time the flame had accelerated enough to produce a blast wave that extensively damaged the plant and houses up to 2 km away (Gugan 1978).

An incident in Franklin county, MO, in 1970 is unique in that the vapor cloud appears to have detonated as a unit. Because a considerable amount of the fuel-air mixture was too rich to detonate, a fireball ensued, burning an area of 14 ha.

Explosions of pressurized vessels containing nonreactive gaseous materials cause massive damage if the contents are at a very high pressure. Although the fragments are not thrown nearly as far as they are with a BLEVE, the blast is more severe, because the entire contents of the vessel contribute to the blast wave. If the vessel is weak, it will rupture at relatively low pressures. A large-scale utility boiler, for example, will "explode" when the internal pressure rises only 1–15 kPa (1.5–2 psig). This pressure rise can be triggered by a combustion explosion in the boiler or by a massive steam leak caused by the rupture of a large tube or header. In this case steam enters the red hot boiler so fast that the normal openings are insufficient to stop the pressure rise. In either case, because of the low L/D ratio of the boiler and its weak structure, the damage to the surroundings is slight, even though the boiler itself may be severely damaged.

Chemical reactor runaway may result from an imbalance in the controlled reaction through loss of adequate cooling, inadequate stirring, the presence of too much catalyst, etc. The pressure buildup is considerably slower than it would be in an explosion due to the detonation of the contents of the container, and the vessel usually ruptures in a ductile mode. If the contents are gaseous, the rupture resembles that of an overpressurized vessel. If the contents are liquid and above the flash-evaporation temperature, as is commonly the case, the explosion resembles a BLEVE.

Physical vapor explosions occur when a finely divided, hot, solid material is rapidly mixed with a much cooler liquid, or when two liquids at different temperatures are violently mixed (Reid 1976). The cooler liquid is converted to vapor so fast that an explosion results from the localized high pressures that are produced. These explosions have been observed when molten material is poured into a container that is moist, and when cryogenic liquid natural gas that contains approximately 10% of a higher hydrocarbon is spilled on water. There is some indication that the mixing of seawater with hot magma may have been responsible for the catastrophic explosions of island volcanoes such as Krakatoa in 1883 and Surtsey in 1963.

Many scenarios have been constructed for the consequences of *nuclear reactor runaway* or core meltdown, including catastrophic breaching of the containment vessel by an internal combustion explosion or a simple pressure burst. Nuclear reactors are constructed in such a way that an accidental upset could not possibly produce anything remotely resembling an atomic bomb explosion. If a nuclear reactor were to explode, the attendant release of long-lived radioactive material would be so disruptive to the local area that the explosion damage, no matter how extensive, would be considered minor. Fortunately, no such accident can be cited because none has occurred, an enviable and unequaled safety record for the first twenty years of commercialization of a new technology.

Research on accidental explosions

Research on accidental explosions has been directed toward determining how the blast waves they produce differ from ideal blast waves, elucidating the explosion process, and devising, developing, and proofing techniques to mitigate their effects and reduce their frequency. Only recently have nonideal explosions been studied in any detail (Strehlow and Baker 1976). It has been shown that nonideal behavior of a source is always directly responsible for any nonideal behavior of the resulting blast wave. A source is nonideal if it has a low energy or power density, if the release of energy is nonspherical, or if it is totally or partially confined by inert material.

Explosions of pressurized vessels and combustion explosions of gases, vapors, and dusts, in or out of enclosures, are examples of explosions of low energy-density sources. The effect of low energy density on the structure of blast waves has been studied rather extensively for bursting spheres, both experimentally and theoretically. Figure 5 shows the evolution of the blast wave from such a bursting sphere.

The effect of slow energy addition, and the concomitant low power density, have been studied for two cases, also illustrated in Figure 5: Adamczyk (1976) studied ramp addition of energy (the addition of energy at a uniform rate throughout the source region), whereas Kuhl and Strehlow and their co-workers (Kuhl et al. 1973; Strehlow et al. 1979) studied flame addition of energy (by central ignition in a spherical source region initially at atmospheric pressure). In a very early piece of work, Taylor (1946) predicted analytically the flow structure for a spherical piston expanding at constant velocity.

It has been found that for spherical source regions low energy and power densities generally cause the overpressure in the blast wave to fall below that predicted by Sachs's scaling on the basis of the energy of the source. It has also been shown that all such nonideal sources yield blast waves, the positive phase impulse of which is equal to that of an ideal explosion of the same total energy.

Nonspherical or directional blast waves are generated by the firing of a gun or rocket, the cracking of a whip, and lightning. There have been a few limited analytic studies, a few numerical studies, and some very specific experimental studies on the effect of nonspherical release of energy on the structure of the blast wave produced. Unfortunately, the analytic studies have all been based on very specialized geometry or the use of approximations that tend to be physically untenable, while the numerical studies have required two-

and three-dimensional hydrocodes that are extremely expensive to run. Thus, generalizations are not currently available. I recently discovered that the overpressure generated by the deflagration of a cloud of arbitrary shape can be estimated by applying a fundamental acoustic principle first stated by Stokes in 1849 (Strehlow, unpubl.), but the full implications of this observation have yet to be examined.

Confinement weakens the external blast wave and causes it to become highly directional. Also, a confined explosion may cause massive internal damage but relatively little external damage, as in explosions in coal mines and some buildings.

Overpressures close to the source are much lower for nonideal than for ideal explosions. If an explosion is deflagrative, no shock wave is formed in the near field (Fig. 5). It was first noted by Rayleigh (1876) that explosions with low power densities produce a blast wave with a sizable negative phase impulse. He inferred this because he sometimes found the glass from a shattered window of a nearby building *outside* the building.

The explosion process is reasonably well understood except for unconfined vapor-cloud explosions. What is not yet understood is how, in cases of soft ignition (i.e. an open flame such as a pilot light), an essentially unconfined flame accelerates sufficiently to produce a damaging blast wave. Prior to 1975, transition to detonation was thought to occur only if a portion of the gas was heated rapidly by compression to its autoignition temperature. Then in 1976, an accidental detonation took place in Wagner's laboratory in Göttingen, under conditions in which compression heating was impossible (Wagner, pers. comm.). Since then, Knystautas and co-workers (1979) have shown that shockless initiation is possible in large-scale eddies formed near obstacles in the flame-induced flow ahead of the flame.

Research into the detonability of natural gas-air mixtures is important, because liquid natural gas is being shipped in bulk (25,000 m^3 tanks, 5 to a tanker), and accidents have the potential for producing extremely large vapor clouds. It is known that direct initiation of detonation in an unconfined cloud of pure methane requires a very large charge of a high explosive, but how large is still a matter of contention. The problem is complicated by the fact that natural gas usually contains a small percentage of higher hydrocarbons, and the addition of about 10% ethane to methane is known to increase its sensitivity to direct initiation considerably.

Venting has been found to be a viable way of limiting damage from explosions in enclosures containing combustible gases, vapors, or dusts, and from runaway chemical reactors (Singh 1978). Bradley and Mitcheson (1978a,b) recently constructed a rather complete theory of venting, and their theoretical estimates approximate closely virtually all the extant laboratory results. However, it has been shown that for gas-air explosions in room-size vessels, the Bradley theory underestimates the maximum internal pressure. Evidently an acoustic instability generated by flame propagation causes higher overpressures than predicted. Such instabilities do not appear in small chambers because their high natural frequencies preclude direct interaction between the acoustic modes and the flame.

Dust explosion venting has been studied extensively by Bartknecht (1978). He finds that for vessels with small L/D ratios and volumes larger than 0.02 m^3, one can define a constant for any substance which is proportional to the maximum rate of pressure rise and which can be used to determine the proper vent area. This approach to the rating of the explosiveness of dust has recently been adopted by the National Fire Protection Association. Bartknecht's work shows definitively that the Hartman bomb, which was used extensively for testing the explosiveness of dust in the 1960s in the United States (Dorsett et al. 1960), is too small to evaluate properly the rate at which the pressure rises, particularly for dusts with a very rapid pressure buildup. Venting dust explosions is quite different from venting gaseous explosions, since there is considerably more combustion outside the enclosure.

In general, venting structures with large L/D ratios (such as the ducting for spray-painting hoods or for dust-collection systems) is much more difficult. It is unnecessary with gases and vapors if enough air is injected to dilute the fuel to a concentration of less than one-quarter of its lean flammability limit (i.e. the largest concentration of fuel and air at which a flame will just fail to propagate over long distances, which is about 1% fuel in air for most higher hydrocarbons). Dusts present a special problem, because if the flow velocity at any point in the system falls below a critical value, the dust settles in the duct, thereby producing a dangerous situation. Requirements for venting ducts are given by the National Fire Protection Association (1978). The principle of chemical reactor venting using a burst disk is well understood if the reactor contains a gas, but not if it contains a flash-evaporating liquid, because of the difficulty of calculating the mass flow and the rate at which the pressure drops.

In contrast to venting, which is a passive technique for the mitigation of the effects of explosions, suppression can be either passive or active. The water barrier method used to suppress coal mine explosions is a typical passive technique (Liebman and Richmond 1974). Most coal mine explosions originate at the working face of the mine and, as is characteristic of explosions in enclosures with large L/D ratios, do not become really dangerous until they have traveled some distance from their point of origin. The water barrier consists of a number of large open tubs of water, which are suspended near the ceiling of the mine a short distance from the working face. The air flow generated by the incipient explosion upsets the tubs and disperses the water. This airborne water acts as a heat sink and quenches the flame. Another passive suppression technique consists of sprinkling the mine with rock dust, usually calcium carbonate from crushed shells. This inert powder is picked up with the coal dust and lowers the temperature enough to quench the flame (Richmond et al. 1979).

Active suppression devices, produced commercially in the United States and West Germany, make use of pressurized bottles containing a dry powder or a halogenated-hydrocarbon extinguishing agent, which are triggered to open by a sensor that is sensitive to either a rise in pressure or

the light emitted by a flame (Liebman et al. 1979).

One way of ensuring that an enclosure will not explode is to make it inert with nitrogen or some other gas. After they are dried, combustion products from boilers are both a suitable and a relatively inexpensive source. The one danger always present is the possibility of suffocation if someone enters the enclosure.

The incidence of BLEVEs can be reduced by the application of intumescent coatings (Cagliostro et al. 1975). Such coatings swell and char readily when heated by an external fire, thereby reducing heat transfer to the substrate, extending the fire life of the object, and reducing the rate at which heat is transferred to the interior. Although there are many adequate intumescent formulations, very few are rugged enough to withstand normal operations of a tank car and the shock of derailment without separating from the surface and leaving large areas unprotected. However, some promising new intumescent materials are now being tested on tank cars in regular service (NTSB 1979).

A study made some years ago showed that virtually all tank car punctures resulting from accidents took place in the bottom third of one end of the car and were caused principally by the coupler on the next car. In 1974 the United States government first required that both ends of tank cars carrying certain hazardous materials be fitted with nonslip couplers and heavy vertical steel plates to protect them from such punctures. A recent study (NTSB 1979) shows that this rather inexpensive retrofit program is proceeding according to schedule, the only major problem being the slow response of some regulatory agencies.

Current status and future needs

Our understanding of accidental explosions has increased tremendously in the past fifteen years, primarily as a result of societal concern. In the United States, for example, the last decade or so has seen new and important involvement in explosion protection by the federal government, insurance underwriters, trade associations, and technical societies. Despite our increased understanding, however, we have not as yet reached—and never will reach—a safety level at which we are entirely free of risk from accidental explosions. If we as a society are dedicated to reducing the risk, we must continue to support research on the causes and mechanisms of explosions as well as on protective devices.

There is, moreover, another aspect to this problem that is equally important. It concerns the level of training, motivation, and general understanding of the people who live and work in our highly technological society. At least 60% of all accidental explosions are caused by human error and not by just mechanical malfunction of equipment. How do you motivate a chemical plant worker to refrain from smoking a cigarette behind a large oil tank where his fellow

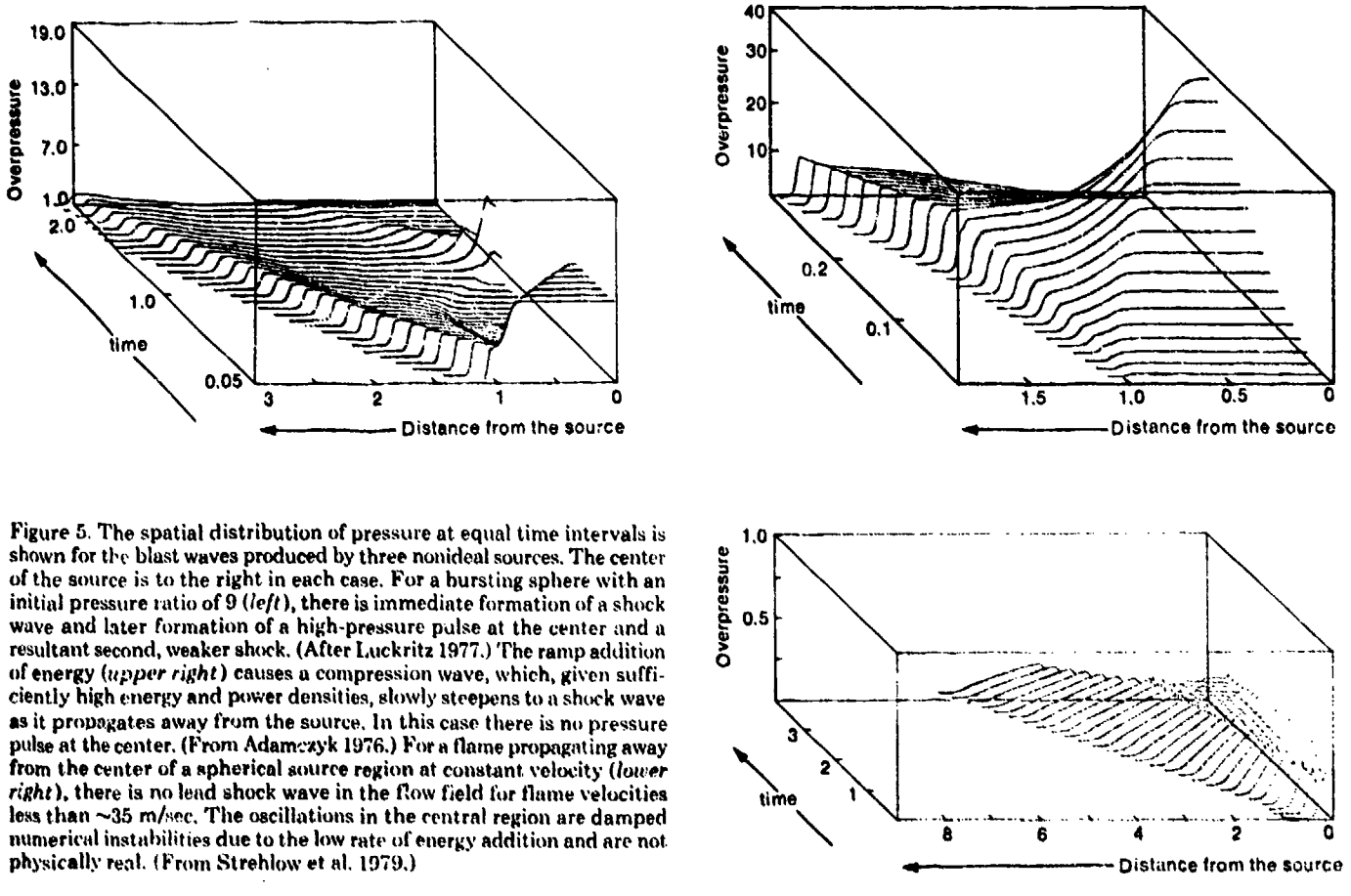

Figure 5. The spatial distribution of pressure at equal time intervals is shown for the blast waves produced by three nonideal sources. The center of the source is to the right in each case. For a bursting sphere with an initial pressure ratio of 9 (*left*), there is immediate formation of a shock wave and later formation of a high-pressure pulse at the center and a resultant second, weaker shock. (After Luckritz 1977.) The ramp addition of energy (*upper right*) causes a compression wave, which, given sufficiently high energy and power densities, slowly steepens to a shock wave as it propagates away from the source. In this case there is no pressure pulse at the center. (From Adamczyk 1976.) For a flame propagating away from the center of a spherical source region at constant velocity (*lower right*), there is no lead shock wave in the flow field for flame velocities less than ~35 m/sec. The oscillations in the central region are damped numerical instabilities due to the low rate of energy addition and are not physically real. (From Strehlow et al. 1979.)

workers cannot see him? How do you train workers to respond appropriately in an emergency situation? How do you teach all the people who sweep down floors and walls in grain elevators that grain dust suspended in air is dangerously explosive? How do you get people to write regulations that reduce risk without imposing an excessive economic burden? These questions and many more like them must be addressed.

It appears that the awareness developed over the past fifteen years will continue to grow. I can see no diminution in the research effort, and I am heartened by the large number of companies and government research agencies that are worried about safety in the work place and in transportation systems. Accidental explosions will certainly continue to occur, and only a continued effort to further our understanding will lead to a reduction in their frequency and impact in the future.

References

Adamczyk, A. A. *An investigation of blast waves generated from nonideal energy sources*. 1975 diss., Univ. of Illinois.

AMCP. 1972. *Engineering Design Handbook. Principles of Explosive Behavior*. AMCP 706-180, Headquarters U.S. Army Material Command.

Baker, W. E. 1973. *Explosions in Air*. Univ. of Texas Press.

Baker, W. E., J. J. Kulesz, R. E. Ricker, R. L. Bessey, P. S. Westine, V. B. Parr, and G. A. Oldham. 1975. *Workbook for Predicting Pressure Wave and Fragment Effects of Exploding Propellant Tanks and Gas Storage Vessels*. NASA CR-134906. NASA Lewis Research Center. Reprint. 1977.

Baker, W. E., P. H. Cox, P. S. Westine, J. J. Kulesz, and R. A. Strehlow. 1978. *A Short Course on Explosions Hazards Evaluation*. San Antonio, TX: Southwest Research Institute.

Baker, W. E., P. S. Westine, and F. T. Dodge. 1973. *Similarity Methods in Engineering Dynamics: Theory and Practice of Scale Modeling*. Rochelle Park, NJ: Spartan Books.

Bartknecht, W. 1978. *Explosionen: Ablauf und Schutzmassnahmen*. Springer.

Bradley, D., and A. Mitcheson. 1978a. The venting of gaseous explosions in spherical vessels. I. Theory. *Combust. and Flame* 32:221–36.

———. 1978b. The venting of gaseous explosions in spherical vessels. II. Theory and experiment. *Combust. and Flame* 32:237–55.

Burgoyne, J. H., and A. D. Craven. 1973. Fire and explosion hazards in compressed air systems. *Loss Prevention* 7:79–87.

Cagliostro, D. E., S. R. Riccitiello, K. J. Clark, and A. B. Shimizer. 1975. Intumescent coating modeling. *J. Fire and Flammability* 6:205–21.

Cybulski, W. 1975. *Coal Dust Explosions and Their Suppression*. Springfield, VA: U.S. Department of Commerce NTIS. Translation TT73-54001.

Dorsett, H. G., Jr., M. Jacobson, J. Nagy, and R. P. Williams. 1960. *Laboratory Equipment and Test Procedures for Evaluating Explosibility of Dusts*. U.S. Bureau of Mines, RI 5624.

Gugan, K. 1978. *Unconfined Vapor Cloud Explosions*. Rigley Wark, England: Inst. of Chem. Eng.

Halvorsen, F. H. 1975. Inerting could prevent some tanker explosions. *Loss Prevention* 9:76–81.

Jarrett, D. E. 1968. Derivation of British explosive safety distances. *Ann. NY Acad. Sci.* 152:18–35.

Knystautas, R., J. H. Lee, I. Moen, and H. G. Wagner. 1979. Direct initiation of spherical detonation by a hot turbulent gas jet. In *Seventeenth Symposium (International) on Combustion*, ed. R. A. Strehlow, pp. 1235–45. Pittsburgh: The Combustion Institute.

Kuhl, A. L., M. M. Kamel, and A. K. Oppenheim. 1973. On flame-generated self-similar blast waves. In *Fourteenth Symposium (International) on Combustion*, ed. J. P. Longwell, pp. 1201–14. Pittsburgh: The Combustion Institute.

Lavoisier, A. 1789. *Elements of Chemistry*. Transl. R. Kerr. Reprint. New York: Dover, 1965.

Lee, J. H., R. Knystautas, and G. G. Buch. 1969. *Theory of Explosions*. Dept. of Mechanical Engineering, McGill Univ. AFOSR Scientific Report 69-3090 TR.

Liebman, I., and J. K. Richmond. 1974. *Suppression of Coal Dust Explosions by Passive Water Barriers in a Single Entry Mine*. U.S. Bureau of Mines, RI 7815.

Liebman, I., J. K. Richmond, R. Pro, R. Conti, and J. Corry. 1979. *Triggered Barriers for the Suppression of Coal Dust Explosions*. U.S. Bureau of Mines, RI 8389.

Luckritz, R. T. An investigation of blast waves generated by constant velocity flames. 1977 diss., Univ. of Maryland.

Newmark, N. M. 1953. An engineering approach to blast-resistant design. *Proc. ASChE* 79, separate No. 309.

NFPA. 1978. *Explosion Venting*. National Electric Codes No. 68, Vol. 14. Boston: National Fire Protection Association.

NTSB. 1972. *Railroad Accident Report, Derailment of Toledo, Peoria, and Western Railroad Company's Train No. 20 with Resultant Fire and Tank Car Ruptures, Crescent City, Illinois, June 21, 1970*. NTSB-RAR-72-2. Washington, D.C.

———. 1976. *Pipeline Accident Report: Consolidated Edison Company Explosion at 305 East 45th Street, New York, NY, April 22, 1974*. NTSB-PAR-76-2.

———. 1979. *Safety Report on the Progress of Safety Modification of Railroad Tank Cars Carrying Hazardous Materials*. NTSB-SR-79-2.

Palmer, K. N. 1973. *Dust Explosions and Fires*. London: Chapman and Hall.

Penny, W. G., D. E. J. Samuels, and G. C. Scorgie. 1970. The nuclear explosive yields at Hiroshima and Nagasaki. *Phil. Trans. Roy. Soc.* 266:357.

Price, D. J., and H. H. Brown. 1922. *Dust Explosions; Theory and Nature of Phenomena, Causes, and Methods of Prevention*. Boston: NFPA.

Rayleigh, J. W. S. 1876. *The Theory of Sound*. Reprint. New York: Dover, 1945.

Reid, R. C. 1976. Superheated liquids. *Am. Sci.* 64:146–56.

Richmond, J. K., I. Liebman, A. E. Bruszak, and L. F. Miller. 1979. A physical description of coal mine explosions. Part II. In *Seventeenth Symposium (International) on Combustion*, ed. R. A. Strehlow, pp. 1257–68. Pittsburgh: The Combustion Institute.

Roggersdorf, W., in cooperation with Badische Anilin und Soda Fabrik Ag. 1965. *In the Realm of Chemistry*, pp. 92–94. Düsseldorf: Econ Verlag.

Sachs, R. G. 1944. *The Dependence of Blast on Ambient Pressure and Temperature*. BRL Report 466. Aberdeen Proving Ground, MD.

Singh, J. 1978. *Identification of Needs and Sizing of Vents for Pressure Relief*. Insurance Technical Bureau, Internal Report No. R 037.

Sperrazza, J. 1951. *Dependence of External Blast Damage to A25 Aircraft on Peak Pressure Impulse*. BRL MR 575 (AD 378275).

Stokes, G. G. 1849. On some points in the received theory of sound. *Phil. Mag.* 34(3): 52.

Strehlow, R. A. 1968. *Fundamentals of Combustion*. Scranton, PA: International Textbook Co. Reprint. Huntington, NY: Krieger.

———. 1973. Unconfined vapor-cloud explosions: An overview. In *Fourteenth Symposium (International) on Combustion*, ed. J. P. Longwell, pp. 1189–1200. Pittsburgh: The Combustion Institute.

———. The blast wave from deflagrative explosions, an acoustic approach. Paper presented at the Fourteenth Loss Prevention Symposium, AIChE, June 8–12, 1980, in Philadelphia.

Strehlow, R. A., and W. E. Baker. 1976. The characterization and evaluation of accidental explosions. *Progress in Energy and Combustion Science* 2(1):27–60.

Strehlow, R. A., R. T. Luckritz, A. A. Adamczyk, and S. A. Shimpi. 1979. The blast wave generated by spherical flames. *Combust. and Flame* 35:297–310.

Swisdak, M. M., Jr. 1975. *Explosion Effects and Properties: Part I.—Explosion Effects in Air*. NSWC/WOL/TR 75-116, Naval Surface Weapons Center, White Oak, Silver Spring, MD.

Taylor, G. I. 1946. The air wave surrounding an expanding sphere. *Proc. Roy. Soc.* A186: 273–302.

U.S. Atomic Energy Commission. 1966. *The Study of Missiles Resulting from Accidental Explosions*. Safety and Fire Protection Bulletin 10. Division of Operational Safety, Washington, D.C.

USCG. 1977. *Marine Casualty Report, S. S. Sansinena (Liberian): Explosion and Fire in Los Angeles Harbor on 17 Dec. 1976 with Loss of Life*. Report No. USCG 16732/71895.

Wheaton, E. L. 1948. *Texas City Remembers*. San Antonio, TX: Naylor.

AIChE Loss Prevention, Vol. 14, 1981

APPENDIX C

Blast Wave from Deflagrative Explosions: an Accoustic Approach

Simple acoustic source theory has been applied to determine the maximum overpressure obtainable by the deflagration of nonspherical clouds. In three dimensions, over-pressure is generated not by the rate of energy addition but by the first-tune derivative of the rate. Therefore, deflagrative combustion of edge-ignited clouds produces markedly less overpressure than central, spherical ignition.

R.A. Strehlow
University of Illinois at Urbana-champaign, Urbana, IL.

The determination of the blast wave produced in free space by the nonspherical combustion of a nonspherical vapor cloud has not been examined in any detail, either analytically, or numerically. The problem is important because at the present time spherical theory is being used to estimate the overpressure for clouds of arbitrary shape and no one knows how conservative this approach is. This paper applies simple acoustic source theory to the deflagrative combustion of a few simple free cloud shapes to determine a first cut estimate of the maximum overpressure that one could expect as a function of cloud size and shape.

THE SIMPLE ACOUSTIC SOURCE

Stokes[1] first showed that a simple source of mass at a point $\dot{m}(t)$ (Units: Kg/sec) generates a sound wave in three dimensions which has an overpressure which is proportional to $\dot{m}(t)$. Specifically, as Lighthill[2] states,

$$p - p_o = \dot{m}\left(t - \frac{r}{a_o}\right)/4\pi r \qquad (1)$$

where $t - \frac{r}{a_o}$ replaces t because the wave is propagating away from the source region at the velocity of sound, a_o. Lighthill also states that at some distance from the source the sound will appear to emanate from a point (i.e., the wave will be very close to spherical) if the quantity $(\omega r/a_o)^2 \ll 1$. Here, ω is the circular frequency of the source of sound and r is a characteristic radius of the source region. Finally, for a source which has a finite duration $\int \dot{m}(t)dt = 0$, and therefore $\int (p-p_o)dt = 0$ in the wave. This means that the acoustic pulse from a source of finite duration must have a negative phase impulse equal to the positive phase impulse. This should be contrasted to the pulse emitted by a finite duration source in a strictly one-dimensional channel. In this case the acoustic overpressure is proportional to $\dot{m}(t)$ and the overpressure in the pulse is always positive everywhere.[1]

Now consider the deflagrative combustion of an unconfined cloud of arbitrary shape. For simple source acoustic behavior the effective rate of mass addition $\dot{m}(t)$ may be replaced by an effective rate of volume addition multiplied by the initial gas density, that is, $\dot{m}(t) = \rho_o \dot{v}(t)$.

However, for deflagrative combustion

$$\dot{m}(t) = \rho_o \dot{v}(t) = \rho_o \left(\frac{v_b - v_u}{v_u}\right) \frac{d}{dt}(S_u(t) \cdot A_f(t)) \qquad (2)$$

where $S_u(t)$ is the effective normal burning

0149-3701/81/3810 $02.00 © 1981 AIChE

velocity, $A_f(t)$ is the effective frontal area of the flame and the ratio $(V_b-V_u)/V_u$ is the new volume produced per unit volume of gas burned at constant pressure. Using the notation of Strehlow et al.[3] $(V_b-V_u)/V_u = \tilde{q}/\gamma_o$. Here, $\tilde{q}$ is an effective dimensionless heat addition. Its relation to the $\tilde{Q}$ of Strehlow et al. is given in Appendix A. Therefore, using the definition of the velocity of sound in an ideal gas and combining Eqs. (1) and (2) yields

$$\bar{p} = \frac{\tilde{q}}{4\pi a_o^2 r} \frac{d}{dt} [S_u(t) \cdot A_f(t)]$$

where $\bar{p}$ is the acoustic overpressure. Equation (3) is a significant relationship. It states that the acoustic overpressure generated by deflagrative combustion in three dimensions is given by the time rate of change of the rate of energy addition rather than the rate of energy addition as it is in strictly one-D flow.

The deflagrative combustion of a cloud generates a sound wave of very low frequency. The period of the sound source in this case is given by $\tau = 2\pi/\omega$ where τ is the burn time. Thus the requirement that the source region is acoustically simple becomes

$$[2\pi(r_m/\tau)/a_o]^2 << 1$$

where r_m is a major dimension of the cloud and approximates the distance traversed by the deflagration wave. Even with distortion and motion due to flame propagation $r/\tau \approx S_u$ and the simple source requirement becomes $4\pi^2 M_{Su}^2 << 1$. If the quantity is to be less than 0.1 for no blast wave distortion S_u will be about 17.5 m/sec before deflagrative behavior produces significant distortion of the blast wave. Even for significantly higher values of S_u the first effect will be only to distort the shape of the blast wave. Higher overpressures than estimated here will not occur until S_u becomes quite large. This limitation of the theory has not been quantified as yet.

APPLICATION IN SPHERICAL GEOMETRY

Two classical problems have been treated in spherical geometry. These are the centrally-ignited, constant-velocity flame[3,4] and the Taylor piston problem.[5] For a constant-velocity flame Eq. (3) reduces to the relation

$$\bar{p} = \frac{\tilde{q}S_u}{4\pi a_o^2 r} \frac{dA_f}{dt} \qquad (4)$$

where r is the distance from the source to the observer. For a growing spherical flame ball

$$A_f = 4\pi r_f^2$$

and

$$\frac{dr_f}{dt} = S_S = S_u \frac{V_b}{V_u}$$

Substituting yields

$$\bar{p} = \frac{2\tilde{q}S_u^2 r_f}{a_o^2 r} \left(\frac{V_b}{V_u}\right)$$

where the r in the denominator must be equal to or greater than r_f. If we let it be equal to r_f, and if we substitute the definition of $\tilde{q}$ given above, we obtain an expression for the acoustic pressure on the unburned side of the flame

$$\bar{p}_f = 2\gamma \left[1 - \left(\frac{V_u}{V_b}\right)\left(\frac{V_b}{V_u}\right)^2\right] M_{Su}^2 \qquad (5)$$

which is identical to Eq. (19) of Strehlow et al..[3]

If we write $r_f = S_S t$ for the flame propagation in Eq. (5) and recall that away from the flame t becomes

$$\left(t - \frac{r}{a_o}\right)$$

Eq. (5) may be written

$$\bar{p} = 2\gamma \left[1 - \frac{V_u}{V_b}\left(\frac{V_b}{V_u}\right)^3 M_{Su}^3 \left(\frac{a_o t}{r} - 1\right)\right] \qquad (7)$$

However, the transformation from a flame to a Taylor spherical piston is

$$M_p = \left[1 - \frac{V_u}{V_b}\right]^{1/3} \frac{V_u}{V_b} M_{Su}$$

Therefore, Eq. (7) reduces to

$$\bar{p} = 2\gamma_o M_p^3 \left\{ \frac{a_o t}{r} - 1 \right\} \qquad (8)$$

where the range on r is $S_p t < r < a_o t$. Equation (8) is identical to the Taylor solution for a spherical piston as $M_p \to 0$ (Eq. (13), Strehlow et al. (3)).

We note that in these equations the rate of flame area growth is proportional to r and the rate of decay of a spherical acoustic pulse is proportional to r^{-1}. Thus, for the spherical case the acoustic pressure remains constant at the flame front and the wave that is generated during flame motion is self-similar in r/t. This is a fundamental acoustic property of a constant-velocity flame that is completely surrounded by combustible material when it burns. It has been verified by numerous theoretical and numerical investigations. (3,4)

APPLICATION TO FREE CLOUDS

We restrict ourselves to clouds of arbitrary shape in free space. To simplify the treatment, we will consider free clouds which have a horizontal plane of symmetry for cloud shape, cloud distortion during deflagration and deflagration wave shape. Since we now wish to simply examine the implications of Eq. (3)for general geometries, we for the moment restrict ourselves to considering only constant velocity flames. This means that Eq. (3) reduces Eq. (4) where S_u is an effective normal burning velocity and r is the distance of an observer from the cloud center.

In general, the evaluation of the dA_f/dt term in Eq. (4) is complicated because during deflagrative combustion the cloud ahead of the flame will move and distort with time. This distortion will cause A_f to be a different function of time than that calculated from purely geometric considerations using a constant velocity flame propagating through a stationary cloud.

In order to determine how to best approximate the effect of such distortion for arbitrary ignition of an arbitrary cloud one must first examine flow behavior in two simple limit geometries; strictly one-dimensional flow caused by deflagration and volumetric heat addition in three dimensions.

The wave diagram for a strictly one-D flow driven by a constant-velocity deflagration wave is shown in Figure 1. If we model the combustion of a stoichiometric methane-air mixture as proposed in Strehlow et al.,(3) the gas to the right of the flame and to the left of the contact surface (regions 0, 1, & 3) can be assumed to have a heat capacity ratio $\gamma_0 = \gamma_1 = \gamma_3 = 1.4$, while the gas in region 2 has a $\gamma_2 = 1.202$. Additionally, the effective value of dimensionless energy addition is $\bar{q} = 8.430$. This means (from Appendix A) that $\theta = 9.242$ and that $V_b/V_u = 7.602$ for constant pressure combustion. Furthermore, for this system the Chapman-Jouguet deflagration Mach number is 0.16631.

The properties of the wave system of Figure 1 were calculated using the shock relationships from Liepman and Roshko(6) for the shocks S_1 and S_3, the deflagration relationship from Strehlow et al.(3) for the flame and the contact surface requirement that $U_{p2} = U_{p3}$ and $P_2 = P_3$. The results of this calculation that are important to this paper are summarized in Figure 2.

Figure 2 shows that particle velocities generated by flame propagation are relatively high and that the apparent flame speed relative to an observer is from 4.3 to 9.3 times the actual normal burning velocity. Also it is less than the space velocity of a spherical flame if the one-dimensional flame is traveling at less than about 0.9 of its maximum (CJ) velocity. Furthermore, the ratio $|U_{p3}/U_{p1}|$ lies between 1.0 and 1.4 in this same velocity range. This last observation simply means that even relatively high speed flame propagation from a free surface in one-dimensional space displaces the gas rather uniformly to the front and back. This is to be constrasted to the behavior of a one-dimensional CJ detonation, which displaces the gas primarily in the direction of detonation propagation.

We now wish to determine what happens if we relax the confinement normal to the flame propagation direction for the case of deflagrative combustion. To estimate this effect we assume that if energy is added relatively slowly to a gaseous volume, the volume will expand an equal distance in all directions. During flame propagation

through a cloud the flame can be assumed to be a relatively thin sheet of energy addition when compared to the cloud dimensions. In other words the flame can be assumed to occupy a volume $A\Delta L$ when $\Delta L << \sqrt{A}$. Under these circumstances one would expect the major expansion to occur in a direction normal to the local orientation of the flame even though the pressure is propagating almost equally in all three dimensions.

This assumption has been qualitatively verified experimentally by observing flame propagation in a propane-air elongated pancake cloud above a flat plate of about 50 mm height and 0.6 m x 0.3 m, edge ignited at the center of the 0.3 m edge.(7) The flame's apparent propagation speed was about 3.5 times the normal burning velocity, and its luminous height was about equal to the initial cloud height. Furthermore the flame flashed to encompass an area considerably larger than the original lateral extent of the cloud. The assumption has also been reasonably well verified by numerical calculations made by Dr. Len Hazelman (8) at Lawrence Livermore Laboratories using a 2 D hydrocode. He calculated flow and flame propagation in an open 2 D channel. His calculations yielded a flame height almost twice the initial cloud height and an apparent flame speed about three times the normal burning velocity. However, his numerical flame had a thickness only one-third of the cloud height and this should lead to more vertical distortion.

These results indicate that for any arbitrary free cloud and igniter geometry in which the flame is not completely surrounded by a combustible mixture one may make the following conservative assumptions about flame-induced distortion.

1. The burning velocity that should be used is S_u. This is because, irrespective of the motion of the flame induced by the flow, the entire cloud will burn in a time, τ, given by $S_u\tau = r_m$ where r_m is the distance from the igniter to the farthest point in the initially quiescent cloud.

2. The increase of flame area in a free cloud due to distortion of the cloud by flame-induced flow will never exceed the value V_b/V_u calculated for isoboric combustion. This is because this is the value of distortion of the unburned material produced during combustion of a completely surrounded (spherical) flame, and relief due to product gas motion away from the flame can only reduce this factor.

Thus the general procedure for determining a first conservative approximation to the effect of cloud shape and igniter location on the overpressure-time behavior in the blast wave when the igniter is not completely surrounded by the cloud is as follows:

1. Assume a value of S_u.
2. Calculate dA_f/dt for a flame traveling at velocity S_u through the quiescent cloud.
4. Correct for distortion by multiplying by V_b/V_u.

Examples for Specific Geometries

a. Central (line) ignition of a pancake cloud.
The flame area is given by

$$A_f = 2\pi r_f H$$

where r_f is the flame radius and H is the height of the pancake. Therefore

$$\frac{dA_f}{dt} = 2\pi H \frac{dr_f}{dt} = 2\pi H S_u$$

and

$$\bar{P}_{max} = \frac{\rho S_u^2 H}{2a_o^2 R_{obs}} \cos\left[\frac{V_b}{V_u}\right] \qquad (9)$$

where R_{obs} is the distance of an observer from the center of the cloud.

b. Edge (line) ignition of a pancake cloud.

The area of a flame propagating from an edge of a cloud of radius R is given in terms of the distance propagated by the formula

$$A_f = 2Hr_f \cos^{-1}\frac{r_f}{2R}$$

Now

$$\frac{dA_f}{dt} = \frac{dA_f}{dr_f} \cdot \frac{dr_f}{dt} = \frac{dA_f}{dr_f} \cdot S_u$$

Therefore

$$\bar{P} = \frac{\rho S_u^2 H}{2\pi a_o^2 r}\left[\cos^{-1}\frac{r}{2R} - \frac{\frac{r}{2R}}{\sqrt{1-\left(\frac{r}{2R}\right)^2}}\right]\left(\frac{V_b}{V_u}\right)$$

or

$$\bar{P}_{max} = \frac{\rho S_u^2 H}{4a_o^2 R_{obs}}\left(\frac{V_b}{V_u}\right) \qquad (10)$$

which is exactly half that predicted for a centrally-ignited pancake.

c. End (point) ignition of an ellipsoid (cigar-shaped) cloud.

Assume a flat flame of location r_f propagates from one end of a long cloud with a minor radius of rotation d and major radius b.

Flame area is therefore

$$A_f = \pi d^2\left[1 - \frac{r_f^2}{b^2}\right]$$

or

$$dA_f = -2\pi r_f \frac{d^2}{b^2}$$

Now let

$$-b = -L/2 \le r \le L/2 = b \quad \text{and} \quad D = 2d$$

where L is the length of the ellipsoid. Therefore

$$\bar{P} = \frac{-\rho S_u^2 D^2}{2a_o^2 r L^2} r_f \left(\frac{V_b}{V_u}\right)$$

and

$$\bar{P}_{max} = \frac{\rho S_u^2}{4a_o^2} \cdot \frac{D}{R_{obs}} \cdot \frac{D}{L}\left(\frac{V_b}{V_u}\right) \qquad (11)$$

Now assume that ρ, S_u, a_o, and (V_b/V_u) are independent of cloud shape and that the observer is at a fixed distance from the center of a cloud of fixed volume but of these different shapes. Call the volumes $V_s = V_p = V_c$, where the subscripts s, p, and c refer to spherical, pancake and cigar shaped clouds, respectively. Also define the aspect ratio of the cloud $\mathcal{AR}$ as $\mathcal{AR}_p = 2R_p/H_p$ and $\mathcal{AR}_c = D_c/L_c$. Using this notation we obtain

$$H_p = D\sqrt{\frac{2}{3\mathcal{AR}}} \qquad (12)$$

and

$$D_c = \frac{D_s}{\sqrt[3]{\mathcal{AR}}} \qquad (13)$$

Combining Eqs. (5), (9), (10) and (11) with Eqs. (12) and (13) yields

$$\left(\frac{\bar{P}_p}{\bar{P}_s}\right)_{max} = \frac{1}{\left[12\left(\frac{\theta}{\gamma_o}+1\right)\mathcal{AR}\right]^{1/3}} \qquad (14)$$

and

$$\left(\frac{\bar{P}_c}{\bar{P}_s}\right)_{max} = \left[\frac{2}{3\left(\frac{\theta}{\gamma_o}+1\right)\mathcal{AR}}\right]^{1/2} \qquad (15)$$

where the factor $\frac{\theta}{\gamma_o} + 1 = V_b/V_u$ arises because we are considering the initial cloud diameter and Eq. (5) is written in terms of the final radius. Eq. (14) is for central-line ignition of a pancake: for edge-line ignition $(\bar{P}_c/\bar{P}_s)_{max}$ is one half of this value.

Figure 3 is a plot of Eqs. (13) and (14). It shows that the deflagration, after edge ignition of a large aspect-ratio cloud, produces much lower overpressures than central ignition of a spherical cloud. It should be pointed out that point ignition of the edge of a free spherical cloud $\mathcal{AR}_c = 1$ would yield a higher overpressure than calculated with Eq. (14) because the derivation of Eq. (11) assumed a flat flame. In reality one would expect a flame of roughly spherical shape to propagate away from a point source and the initial rate of flame area increase would be larger in this case than for a flat flame.

EFFECT OF CLOUD SIZE

Equation (3) can be used to give an order of magnitude estimate of flame areas and accelerations that are necessary for a deflagration to produce a damaging blast wave. If we define the threshold of damage to be 0.1 Bar and assume that this level of overpressure is to be produced 100 m from the cloud center in an atmosphere with a velocity of sound of 350 m/s, Eq. (3) reduces to

$$1.6 \times 10^7 = A_f \frac{dS_u}{dt} + S_u \frac{dA_f}{dt} \qquad (16)$$

Table I was constructed from Eq. (16) under the two limit assumptions that (1) $dS_u/dt = 0$ and (2) $dA_f/dt = 0$.

Notice from Table I that even for very high flame velocities the rate of flame area increase must also be very high if even a weak blast wave is to be generated. On the other hand, only extremely large initial flame areas, exhibiting very large flame acceleration over their entire frontal area are necessary to produce a weak blast wave from deflagrative combustion. Both of these observations imply that extremely large clouds are required if one is to produce significant overpressure by deflagrative combustion alone.

DISCUSSION AND CONCLUSIONS

The application of simple source acoustic theory to deflagrative combustion of an unconfined cloud shows that:

1) It is very difficult to produce a damaging blast wave by deflagrative combustion once the flame is not completely surrounded by a combustible mixture.

2) The maximum overpressure produced, other circumstances being equal, is proportional to the ratio of the minor dimension of the cloud to the distance to the observer.

3) Blast pressure is rather uniformly distributed in all directions, i.e., the blast is roughly spherical.

4) The cloud must be very large if a damaging blast wave is to be produced.

5) Spherical flame propagation calculations such as those of Kuhl *et al.* and Strehlow *et al.* greatly overestimate blast pressures from deflagrative combustion following edge ignition of clouds with large aspect ratios.

From various accident accounts of the sequence of events that led to the production of a damaging blast wave after delayed ignition of a massive spill of combustible material it appears that:

1) There is a threshold spill size below which blast damage does not occur. Gugan's[9] documentation of incidents shows that blast damage has been observed for spills of less than 2000 Kg but more than 100 Kg only for the fuels H_2, H_2-CO mixture, CH_4 and C_2H_4. Blast damage has been recorded only for spills greater than 2000 Kg for all other fuels.

2) In the majority of cases where blast

TABLE I

(1) $dS_u/dt = 0$		(2) $dA_f/dt = 0$	
S_u, m/s	$\frac{dA_f}{dt}$, m^2/s	A_f, m^2	$\frac{dS_u}{dt}$, m/s^2
1	1.7×10^7	100	1.7×10^5
10	1.7×10^6	10,000	1.7×10^3
100	1.7×10^5	1,000,000	17

damage occurred, fire was present for a considerable period before the blast occurred. 3) In many cases damage is highly directional.

These observations when coupled with the results of simple source acoustic theory for deflagrative combustion lead to the following conclusions.

1. There should be a size threshold below which blast will not occur as long as ignition is "soft", i.e., does not directly trigger detonation.

2. The fact that fire is present early after ignition indicates that massive flame accelerations are necessary to lead to blast wave formation. Since the flame must have burned through the cloud edge by the time the blast is produced, simple acoustic source theory must be operative for even high deflagration velocities. Thus, the blast must arise from some sort of effectively supersonic combustion process or from very rapid increases in effective surface area of the flame.

3. Simple acoustic source theory for deflagrative combustion shows that deflagrative processes per se cannot produce highly directional effects. However, it is well known that detonative combustion of a cloud does produce highly directional blast wave effects.

LITERATURE CITED

1. Stokes, Phil. Mag. XXXIV, Ser. 3, p. 52. (1849)
2. Lighthill, J., Waves in Fluids, Chapter 1, Cambridge Univ. Press, Cambridge (1978).
3. Strehlow, R.A., Luckritz, R.T., Adamczyk, A.A., and Shimpi, S.A., "The Blast Wave Generated by Spherical Flames", Combustion and Flame 35, 297-310 (1979).
4. Kuhl, A.L., Kamel, M.M., and Oppenheim, A.K., Fourteenth Symposium (International) on Combustion, The Combustion Institute, Pittsburgh, 1973, pp. 1201-1215.
5. Taylor, G.I., Proc. Roy. Soc. A 186, 273-292 (1946).
6. Liepman, H.W. and Rosnko, A., Elements of Gas Dynamics, Chapter 3, p. 62, Wiley, New York, (1957).
7. Huseman, P., Private communication, Urbana, IL (1979).
8. Hazelman, L., Private communication, Livermore, CA (1979).
9. Gugan, K., Unconfined Vapour Cloud Explosions, The Institute of Chemical Engineers, London (1979), pp. 28-35, 39.

ACKNOWLEDGMENTS

The author wishes to thank Dr. Le Hazelman of Lawrence Livermore Laboratory, Livermore, California, for performing some 2 D hydrocode calculations. He also wishes to thank Mr. Peter Huseman for performing a few critical experiments and Dr. Harold O. Barthel for a number of helpful discussions.

This work was supported by Arthur D. Little, Inc. and by AFOSR Grant 77-3336, Dr. B. T. Wolfson, Technical Monitor.

APPENDIX A

The Generalized Heat Addition Hugoniot

Strehlow et al.(3) have shown that a generalized heat addition Hugoniot quite accurately fits the real Hugoniot for hydrocarbon-air combustion over the range of interest for vapor cloud explosions. Briefly they assume that

$$H_o = C_{p_o} T$$

and

$$h_1 = C_{p_1} T - \tilde{Q}$$

where $\tilde{Q}$ is the energy added at the deflagrative/detonative discontinuity and C_{p_o} and C_{p_1} are different heat capacities for the reactive and product gases respectively.

Using this approach they define a dimensionless energy addition as

$$\tilde{q} = (\gamma_1 - 1)\tilde{Q}/P_o V_o$$

Thus the volume change for constant pressure combustion is given by the expression

$$\frac{V_b - V_u}{V_u} = \frac{(\gamma_1 - \gamma_o)}{\gamma_1(\gamma_o - 1)} + \frac{\tilde{q}}{\gamma_1}$$

therefore

$$\frac{V_b - V_u}{V_u} = \frac{(\gamma_1 - \gamma_o)}{\gamma_1(\quad)}$$

Now define

$$\frac{V_b - V_u}{V_u} = \frac{\hat{q}}{\gamma_o}$$

for ease of nondimensionalizing the acoustic problem. This yields

$$\hat{q} = \frac{\gamma_o(\gamma_1 - \gamma_o)}{\gamma_1(\gamma_o - 1)} + \frac{\gamma_o}{\gamma_1}\tilde{q}$$

For stoichiometric methane-air mixtures[3]

$$\gamma_o = 1.4 \qquad \gamma_1 = 1.202 \quad \text{and} \quad \tilde{q} = 8.430$$

Therefore

$$\frac{V_b - V_u}{V_u} = \frac{\hat{q}}{\gamma_o} = 6.6015$$

Thus $\hat{q} = 9.242$

and $\dfrac{V_b}{V_u} = 7.6015$

for a stoichiometric methane cloud.

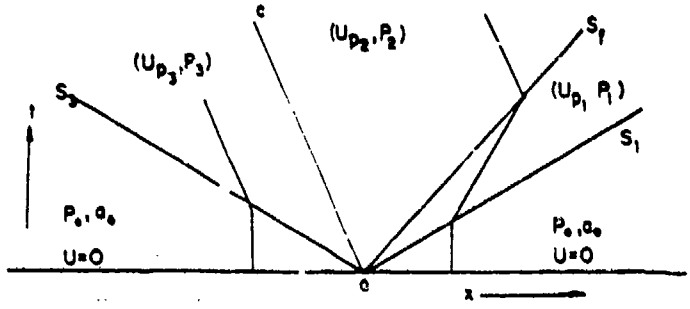

Figure 1. The wave diagram for strictly one-dimensional, constant-velocity deflagration of a free cloud after edge ignition (edge located at $x = 0$, S_f is apparent flame speed).

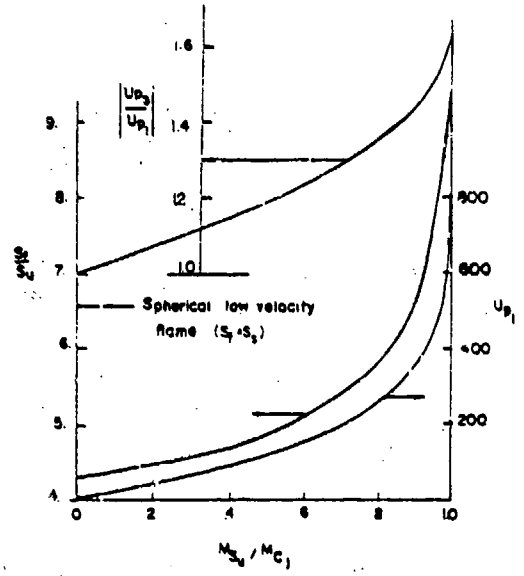

Figure 2. Flow velocities and apparent speeds associated with strictly one-dimensional deflagration combustion illustrated in Figure 1.

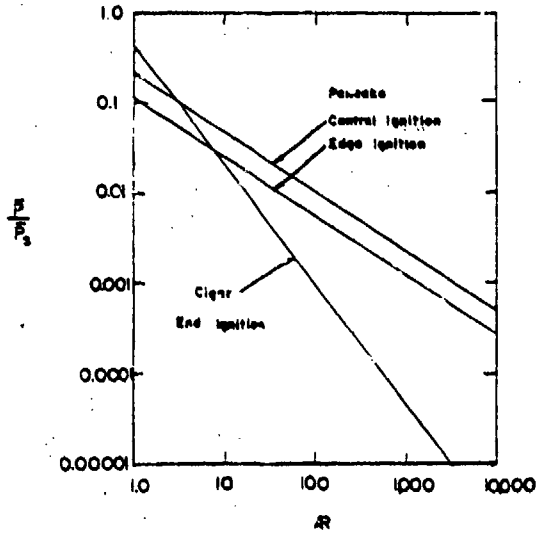

Figure 3. Effect of the aspect ratio, $\mathcal{R}$, on the maximum blast wave pressure rise for the deflagrative combustion of pancake and cigar-shaped clouds. Cloud volume, normal burning velocity and observer distance from cloud center all assumed to be constant from cloud to cloud.